

Satellite Conjunction Monte Carlo Analysis

Salvatore Alfano*

Center for Space Standards and Innovation, Colorado Springs, Colorado, 80920

This work uses a simplified Monte Carlo process to assess the satellite collision probability computations of various methods and to obtain a preliminary estimate on their bounds of utility. The process starts with a simple two-body analytical propagation of the position and velocity vectors and their associated 6x6 covariance from epoch to the time of closest approach (TCA). Each object is assumed spherical and a time span is set about the initial TCA to bound the results. No assumptions are made regarding the constancy or direction of the relative velocity over the encounter's time span. The epoch vectors are randomly perturbed in accordance with the initial covariance matrix values and a collision determination made if the relative distance at any time in the span is equal to or less than the combined object radius. Two statistical bounding criteria are used to determine the minimum number of cases needed. The Monte Carlo results are then compared to probability computations that use the unperturbed orbital data at TCA. This particular work does not attempt to simulate real-world perturbations such as atmospheric drag and/or various gravity fields, but rather assures the consistency of the Gaussian process from epoch to closest approach point for the chosen force model. Because no unique or complicated force models are used the results can be easily repeated and independently validated.

* Senior Research Astrodynamist, CSSI, 7150 Campus Drive, Suite 260, Colorado Springs, CO, 80920-6522, salfano@centerforspace.com, AIAA Associate Fellow.

Nomenclature

C3	=	3x3 combined positional covariance matrix
C6	=	6x6 position/velocity covariance matrix
dt	=	time step
ECI	=	Earth Centered Inertial frame
erf	=	error function
f	=	Patera's aspect ratio
f _{pt}	=	fractional probability threshold
m	=	combined covariance ellipsoid scale factor
n	=	number of independent Monte Carlo trials alternately the number of radial or circumferential divisions
OBJ	=	cross-sectional radius
P	=	probability
\hat{P}	=	estimated probability from Monte Carlo simulation
P _T	=	True probability
r	=	relative distance vector
R	=	radius of torus (alternately Patera's distance to combined object center)
TCA	=	time of closest approach
t _i	=	start time
t _f	=	end time
V	=	swept out volume of collision tube
x _m	=	rotated x position of combined object center
y _m	=	rotated y position of combined object center
α	=	angle between the object's distance vector and the covariance ellipse's x axis
δ	=	Statistical confidence parameter
ε	=	Statistical error measure (alternatively Patera's covariance-centric angle)
Φ	=	error state transition matrix
ρ	=	combined object radius
σ	=	standard deviation
θ	=	object-centric angle

I. Introduction

There are numerous methods in use for computing satellite collision probability (COLA) where the relative motion is assumed linear¹⁻⁷. The relative speed and accuracy of these methods have been compared in a previous work⁸. Such methods perform their analysis with the objects modeled as spheres, thus eliminating the need for attitude information. Their relative motion is considered linear for the encounter by assuming the effect of relative acceleration is dwarfed by that of the velocity. The positional errors are assumed to be zero-mean, Gaussian, uncorrelated, and constant for the encounter. The relative velocity at the point of closest approach is deemed sufficiently large to ensure a brief encounter time and static covariance. The cumulative collision probability P is found by integrating the three-dimensional, Gaussian, relative position density over the volume V (collision tube) that is swept out by the combined hardbody of the two space objects over a specified time interval (t_i, t_f)

$$P = \frac{1}{\sqrt{8 \cdot \pi^3} \cdot \sigma_x \sigma_y \sigma_z} \int_{t_i}^{t_f} \int \int \exp \left[\frac{-x^2}{2 \cdot (\sigma_x)^2} + \frac{-y^2}{2 \cdot (\sigma_y)^2} + \frac{-z^2}{2 \cdot (\sigma_z)^2} \right] dx dy dz \quad (1)$$

The probability density in the bracketed section is conveniently represented in the diagonal frame of the relative position-error covariance matrix. The definition of the integration volume $V(t_i, t_f)$ is the most complicated aspect of evaluating Equation 1. Coupled with object sizes, the encounter region determines the limits of integration. The region is defined when one object is within a standard deviation (σ) combined covariance ellipsoid shell scaled by a factor of m . This user-defined, three-dimensional, $m\text{-}\sigma$ shell is centered on the primary object; m is typically in the range of 3 to 8 to accommodate conjunction possibilities ranging from 97.070911% to 99.999999%.

The assumption of linear relative motion may not be valid in all cases. Chan⁹ and Alfano¹⁴ proposed test criteria for nonlinearity. Chan⁹, Patera¹⁰, Alfano^{11,14}, and McKinley¹² proposed different methods for calculating collision probability for such instances. Nonlinear motion is typically associated with long-term encounters which imply the covariance can no longer be assumed static. The collision tube will not be straight, invalidating the simple dimensional reduction used for linear motion. The size of the $m\text{-}\sigma$ shell must also be carefully considered, especially if the relative motion reverses direction during the encounter.

This paper assesses the satellite collision probability computations of several of the aforementioned methods. A simple two-body analytical propagator is used to move the position and velocity vectors and their associated 6x6 covariance from epoch to the time of closest approach (TCA). A time span is set about the initial TCA to bound the results. The epoch vectors are randomly perturbed in accordance with the initial covariance matrix and a collision determination made if the relative distance at any time in the span is equal to or less than the combined object radius. A statistical bounding criterion is used to determine the minimum number of cases needed. The Monte Carlo results are then compared to probability computations that use the unperturbed orbital data at TCA. There is no attempt made to simulate real-world perturbations such as atmospheric drag and/or various gravity fields. This analysis is simply meant to demonstrate the consistency of the Gaussian process from epoch to closest approach point for the chosen force model.

For linear relative motion, Patera's and Alfano's methods are assessed. The Patera⁷ model is based on a one-dimensional probability density function (pdf) and is formulated as a line-integral. Its evaluation is performed numerically by taking short line segments around a closed contour. The Alfano⁶ model is also based on a one-dimensional pdf expressed as two error functions and one exponential term. It is numerically evaluated using well-developed software for error functions.

For nonlinear relative motion three methods are assessed. The first adjoins right cylinders (tubes) in Cartesian space using an extension of Patera's linear method. For each time step the tube sections are sufficiently small enough so that, over the interval, the relative motion can be assumed linear and the covariance constant. At every time step the objects, their positions, and their covariances are transformed to the primary object's body frame and the tube section's probability is calculated. Adjoining right cylinders may produce gaps and overlaps where the tube sections meet. The second method addresses these gaps and overlaps by representing each tube section as a bundle of abutting parallelepipeds¹⁴ of differing lengths to create a compound miter with the neighboring tube. This is

accomplished by incorporating the error functions of Alfano's method. The third method uses voxels¹¹ to model the combined object as it travels through the tube.

II. Monte Carlo Methodology

The Monte Carlo process in this analysis requires a six-by-six position/velocity covariance matrix for each satellite at their respective epochs. The procedure first determines the rotation matrix that diagonalizes the covariance matrix. The standard deviations from the diagonal matrix are used to randomly produce six perturbations which are then rotated back to the original frame and added to the epoch states. In a manner similar to Chao¹⁵ these perturbed states are propagated about a time spanning the TCA as set by the user. For this study the span is one-quarter of the primary object's orbital period forward to one-quarter back from TCA. A collision determination is made if the relative distance at any time in the span is equal to or less than the combined object radius. To accomplish this, relative distance interpolation is performed using the ANCAS¹⁶ method of localized cubic polynomials. Two statistical bounding criteria are used to determine the minimum number of cases needed. No assumption is made regarding the constancy or direction of the relative velocity over the encounter's time span, so this Monte Carlo process applies to nonlinear relative motion as well as linear.

A. Bounded Random Sampling

We wish to validate how random variations of the epoch states affect our conjunction assessment. To accomplish this we can analyze uncertainty propagation using a Monte Carlo method by comparing our computed probability with a sufficient ensemble of sampled estimates. First, we assume that deviations to the initial states are randomly distributed, Gaussian, zero mean, and shaped by the epoch covariance. Second, we must characterize the number of random realizations required to infer the global statistics of the parameter space. The works of Chernoff⁸, Hoeffding¹⁹, and Dagum et al²⁰ provide that characterization. What follows are two ways to determine how many non-adaptive (random) sets of variations are needed to ensure a specified quality of answer.

Chernoff showed that an upper bound can be determined for the probability that an event in a random sample differs significantly from the true probability of the event. Hoeffding extended Chernoff's work by providing a more general bound on how the sample mean of independently and identically distributed random variables deviates from the actual mean.

We wish to find the probability that the Monte Carlo aggregated, multiple-realization, probability estimate \hat{P} is close to the true conjunction probability P_T for n number of independent random trials. The desired level of absolute error (accuracy) is represented by ϵ where $(0 < \epsilon < 1)$. Hoeffding showed that

$$P[\hat{P} > (P_T + \epsilon)] \leq e^{(-2 \cdot n \cdot \epsilon^2)} \quad (2a)$$

and

$$P[\hat{P} < (P_T - \epsilon)] \leq e^{(-2 \cdot n \cdot \epsilon^2)} \quad (2b)$$

We wish to know how reliably our ensemble of Monte-Carlo simulations approximates the true solution. To do this we set a confidence level of $(1-\delta)$ such that

$$P(|\hat{P} - P_T| \leq \epsilon) > 1 - \delta \quad (0 < \delta < 1) \quad (3)$$

The left side of the equation is then represented by component parts

$$P\left(\left|\hat{P} - P_T\right| \leq \varepsilon\right) = 1 - P\left[\hat{P} > \left(P_T + \varepsilon\right)\right] - P\left[\hat{P} < \left(P_T - \varepsilon\right)\right] \quad (4)$$

Substitution of the Hoeffding inequalities yields

$$\delta > 2e^{-2 \cdot n \cdot \varepsilon^2} \quad (5)$$

which leads to the general expression

$$n > \frac{1}{2 \cdot \varepsilon^2} \cdot \ln\left(\frac{2}{\delta}\right) \quad (6)$$

In summary, the Chernoff-Hoeffding bound can be used to determine a sufficient number of Monte Carlo simulations (n) required to achieve a given accuracy (ε) with a confidence level of $(1-\delta)$. This result is not specific to satellite conjunction analysis and can be applied to any problem where statistical sampling is used to approximate solutions to quantitative problems. As an example, to meet a 1% relative accuracy for a P_T of 0.3 ($\varepsilon=0.003$) with a 95% confidence level ($\delta=0.05$), at least 204,938 independent, random simulations are needed. Figure 1 is provided for the reader's convenience to determine a sufficient number of runs for a given probability using this bounding method. The number of samples required to guarantee high confidence is inversely proportional to the square of actual probability. Therefore, a small true probability will require a large number of samples to achieve a specific confidence level.

Dagum et al²⁰ determined that the number of samples could be significantly reduced under certain conditions. With knowledge of the expected value of P_T but not its variance, if

$$\varepsilon \leq (1 - P_T) \cdot P_T \quad (7)$$

then the upper bound can be represented by

$$n > \frac{4 \cdot (e - 2) \cdot \left[(1 - P_T) \cdot P_T\right]}{\varepsilon^2} \cdot \ln\left(\frac{2}{\delta}\right) \quad (8)$$

For small values of ε the condition is easily satisfied when P_T is not near one. As seen in Figure 1, the number of samples required to guarantee high confidence becomes inversely proportional to the actual probability. Dagum bounding criteria can be used if the true probability can be estimated apriori.

B. Propagation

Two-body analytical propagation of position, velocity, and covariance is done using universal variables as explained in Herrick¹⁷. The six-by-six covariance $C6$ is propagated in a single step through the equation

$$C6(t) = \Phi(t) \cdot C6(t_0) \cdot \Phi(t)^T \quad (9)$$

The error state transition matrix (Φ) is described by Vallado¹³ and consists of the partial derivatives of the state at time t with respect to the epoch at t_0 .

$$\Phi(t) = \begin{pmatrix} \frac{\partial \vec{r}_t}{\partial \vec{r}_{t_0}} & \frac{\partial \vec{r}_t}{\partial \vec{v}_{t_0}} \\ \frac{\partial \vec{v}_t}{\partial \vec{r}_{t_0}} & \frac{\partial \vec{v}_t}{\partial \vec{v}_{t_0}} \end{pmatrix} \quad (10a)$$

where each of the elements in Equation 10a is a three-by-three matrix, e.g.,

$$\frac{\partial \vec{r}_t}{\partial \vec{r}_{t_0}} = \begin{pmatrix} \frac{\partial x}{\partial x_0} & \frac{\partial x}{\partial y_0} & \frac{\partial x}{\partial z_0} \\ \frac{\partial y}{\partial x_0} & \frac{\partial y}{\partial y_0} & \frac{\partial y}{\partial z_0} \\ \frac{\partial z}{\partial x_0} & \frac{\partial z}{\partial y_0} & \frac{\partial z}{\partial z_0} \end{pmatrix} \quad (10b)$$

The analytical partial derivatives for the above expressions are also defined in Herrick. If desired, one can extend this method by using detailed force models in determining these equations with analytical or numerical methods. To ensure consistency, the exact models that are used to propagate the orbit must be used to determine the partial derivatives that make up the error state transition matrix.

C. Collision determination

A collision determination is made if the relative distance at any time in the span is equal to or less than the combined object radius. To accomplish this, relative distance interpolation is performed using the ANCAS¹⁶ method of localized polynomials. An ephemeris for each satellite is generated over the desired time span in increments small enough to ensure sub-meter accuracy. A step size of 10 seconds was deemed adequate for GEO, 5 seconds for MEO and 1 second for LEO. The resulting ephemerides are differenced to create a table of relative distances that are evenly spaced in time.

Starting from the unperturbed TCA, four consecutive distances are examined to check if a minimum has occurred in this initial sub-interval. If so, the ANCAS routine computes the minimum distance. If not, then a determination is made whether to increment or decrement time to cause the distance to decrease. Each new value is compared to the previous; if the distance begins to increase, the last four consecutive distances are fed to the ANCAS routine. If the resulting minimum distance is less than or equal to the combined object radius then a hit is recorded.

D. Implementation

Three-dimensional position and velocity data of each object, as well as their six-by-six covariance matrices, are required with the assumption that all starting data are in the Earth Centered Inertial (ECI) frame. Suitable incremental limits should be set for the intermediate time step (dt) with the user specifying the computational stopping condition in terms of time span to/from TCA. The computational algorithm is as follows.

Initially propagate both satellites to determine the unperturbed Time of Closest Approach (TCA)

For each satellite create a series of perturbed ephemerides:

- Determine the six-by-six rotation matrix to diagonalize the epoch covariance matrix
- Randomly assign six perturbations based on the standard deviations of the diagonal covariance matrix
- Apply the inverse rotation to the perturbations and add to the original epoch position and velocity
- Generate an ephemeris according to user-defined time span about unperturbed TCA
- Store the ephemeris
- Repeat as many times as necessary (at least the square root of the number of desired samples n)

Begin Monte Carlo assessment for each pairing of the two sets of stored ephemerides

- Difference the ephemerides at TCA and determine relative distance $D(TCA)$
- Difference the ephemerides at $(TCA-dt)$ and determine relative distance $D(TCA-dt)$
- Difference the ephemerides at $(TCA-2dt)$ and determine relative distance $D(TCA-2dt)$
- Determine time step direction to reduce next distance based on trend of computed distances
- If direction is positive then compute $D(TCA+dt)$, else compute $D(TCA-3dt)$
- Continue moving in this direction until new distance is greater than previous distance
- Use ANCAS and last four consecutive distances to determine minimum distance
- If minimum distance is less than or equal to the combined hardbody radius then record hit

III. Methods Tested

A total of five methods were compared to the Monte Carlo results. Two of the methods were originally developed to compute collision probability for short-term encounters between space-borne objects. The model developed by Patera⁷ is based on a one-dimensional pdf and is cast in the form of a line integral. Its evaluation is performed numerically by taking short line segments around a closed contour. The Alfano⁶ model is also based on a one-dimensional pdf expressed as two error functions and one exponential term and is numerically evaluated.

Two of the methods for long-term (nonlinear) encounters involve breaking the relative path into sufficiently small tubes or parallelepipeds such that the sectional motion is nearly linear, computing the linear-motion probability associated with each section, and then summing. The first of these methods considers each tube to be cylindrical with its ends perpendicular to its axis; this does not account for gaps or overlaps of abutting cylinders. The second method is more complex, using bundled, rectangular parallelepipeds to eliminate these gaps and overlaps by treating the junctions as compound miters while incorporating probability density variations. The third method sections the probability density space into sufficiently small units of volume¹¹ (voxels) where the probability of each voxel touched by the object is summed to produce the overall collision risk.

In addition, a test for linearity¹⁴ is implemented. A fractional probability threshold of 1% is chosen and the approximate minimum relative velocity is found that ensures sufficiency. The threshold is compared to the actual fraction relating linear to nonlinear probability. For the nonlinear cases, the minimum relative velocity should exceed the actual. All test input data and results are contained in Appendix A.

A. Testing for linearity

This test¹⁴ determines when the relative motion is sufficiently linear. This is done by finding the approximate minimum relative velocity needed at the time of closest approach (TCA) to ensure that a pre-specified probability difference will not be exceeded either forward or backward in time while the $m\text{-}\sigma$ shell is traversed. The user defines a fractional probability threshold (fpt) that is within accuracy requirements for intended operations; fpt is the absolute difference between the linear and nonlinear results divided by the linear results. Initially a coarse assessment is performed only on the covariance growth using simple, two-body, orbital dynamics to approximate the bounds of linear motion based on the threshold fpt. This bounding is followed by a refined assessment using the full force models to predict relative orbital motion and covariance changes. The minimum relative velocity is then determined to ensure the fractional probability threshold will not be exceeded. The linear motion assumption is valid if the encounter's relative velocity exceeds the minimum. This test should be done for each and every conjunction as it does not produce an all-encompassing, one-size-fits-all, minimum velocity.

B. Patera's Method

Patera⁷ developed a mathematically equivalent model to Equation 1 as a one-dimensional line integral where r is the distance to the hardbody perimeter and ϵ is the covariance-centric angular position measured from the x-axis.

The probability density is symmetrized enabling the two-dimensional integral to be reduced to a one-dimensional path integral, resulting in the expression

$$P = \frac{1}{2\pi} \oint_{\text{perimeter}} \left(1 - \exp\left(\frac{-r^2}{2\sigma^2}\right) \right) d\epsilon \quad (12)$$

where P is the collision probability and σ is the symmetrized position error standard deviation (σ_x).

Patera then improved his method by switching the integration variable to center it on the object. He oriented the frame to place the combined object center at (R, 0) with α defining the angle between the object's distance vector and the covariance ellipse's x axis. He again symmetrized the space using σ_x and defined θ as the object-centric angle. The reformulation reduced intermediate complexities and also resulted in substantially fewer integration steps to achieve a given level of accuracy. This improved, object-centric method is expressed in integral form as

$$P = \frac{1}{2\pi} \int_0^{2\pi} \left(\frac{f\rho^2 + Rf\rho \cdot \cos(\theta) + Rf \frac{d\rho}{d\theta} \cdot \sin(\theta)}{r^2} \right) \cdot \left(1 - \exp\left(\frac{r^2}{2\sigma^2}\right) \right) d\theta \quad (13)$$

where ρ is the combined object radius, f is the ratio of the covariance matrix's σ_x to σ_y , and r^2 is expressed as

$$\begin{aligned} r^2 = & (R + \rho \cdot \cos(\theta))^2 \cdot (\cos(\alpha)^2 + f^2 \cdot \sin(\alpha)^2) + \rho^2 \cdot \sin(\theta)^2 \cdot (\sin(\alpha)^2 + f^2 \cdot \cos(\alpha)^2) \\ & + 2\rho \cdot (1 - f^2) \cdot \cos(\alpha) \cdot \sin(\alpha) \cdot \sin(\theta) \cdot (R + \rho \cdot \cos(\theta)) \end{aligned} \quad (14)$$

Simple numerical methods require only two sine and two cosine evaluations regardless of the number of integration steps.

C. Alfano's Method

Alfano⁶ developed a series expression to represent Equation 1 as a combination of error (erf) functions and exponential terms. In the encounter plane, the combined object center's location is (xm, ym) with associated standard deviations σ_x and σ_y and combined object radius OBJ. The series expression is given as

$$P = \frac{\text{OBJ} \cdot 2}{\sqrt{8\pi} \cdot \sigma_x \cdot n} \sum_{i=0}^n \left[\text{erf} \left[\frac{\left[ym + \frac{2 \cdot \text{OBJ}}{n} \cdot \sqrt{(n-i) \cdot i} \right]}{(\sigma_y \cdot \sqrt{2})} \right] + \text{erf} \left[\frac{\left[-ym + \frac{2 \cdot \text{OBJ}}{n} \cdot \sqrt{(n-i) \cdot i} \right]}{(\sigma_y \cdot \sqrt{2})} \right] \right] \cdot \exp \left[\frac{\left[\frac{\text{OBJ} \cdot (2 \cdot i - n)}{n} + xm \right]^2}{2 \cdot \sigma_x^2} \right] \quad (15a)$$

The method then breaks the series into m-even and m-odd components and makes use of Simpson's one-third rule. An expression to determine a sufficiently small number of terms is given as

$$m = \text{int} \left(\frac{5 \cdot \text{OBJ}}{\min(\sigma_x, \sigma_y, \sqrt{xm^2 + ym^2})} \right) \quad (15b)$$

with a lower bound of 10 and upper bound of 50.

D. Method of Adjoining Cylinders

The method of adjoining right cylinders¹⁴ begins with object position and velocity data at the time of closest approach. Propagation is done forward/backward in time until a user limit is reached as previously described. For each time step the tube sections should be sufficiently small enough so that, over the interval, the relative motion can be assumed linear and the covariance constant. For each section, a two-dimensional probability is computed by projecting the combined object shape onto a plane perpendicular to the relative velocity. In addition, a one-dimensional probability is computed along the relative velocity vector by determining the component position from the mean at each end of the tube and then dividing by the standard deviation for that axis, thus producing each endpoint's Mahalanobis distance. The product of these probabilities yields the sectional probability. All sectional probabilities are summed until the time and/or sigma limit is reached. The probability of each cylinder is determined by multiplying the two-dimensional linear-motion probability by the sectional (relative velocity axis) probability. For this study Patera's linear-motion probability model⁷ was used for each section.

The tubes have no gaps when dealing with linear relative motion. For such cases, the nonlinear results should match the linear-motion probability for constant covariance. As seen in Figure 2, nonlinear motion causes gaps and overlaps where the tube sections meet. The amount of error will vary based on the degree of bending/overlap relative to probability density.

E. Method of Bundled Parallelepipeds

The cylinders described in the previous section are replaced by bundles of abutting parallelepipeds¹⁴. Each parallelepiped end is adjusted to form a compound miter where neighboring tubes meet, thereby reducing gaps and overlaps. The approach that follows applies to all relative motion and is coupled with a modified error-function method⁶ to allow any object shape. As before the method begins with object position, velocity, and covariance data at TCA. Propagation is done forward/backward in time until a user limit is reached. For each time step the tube sections are sufficiently small enough so that, over the interval, the relative motion can be assumed linear and the covariance constant. The probability of each parallelepiped is computed and summed to obtain the overall probability of the tube section. All sections are summed to produce the overall encounter probability.

F. Method of Voxels¹¹

The complete spherical object is transformed into Mahalanobis space at discrete times while assuring that the time increment is sufficiently small so that no volume units are skipped between time frames. An assessment is then made to determine what voxels are contained within the combined, transformed, translated object. If any of those voxels were contained in previous iterations, they are eliminated from further consideration because they have already been accounted for. The probabilities of the remaining (new) voxels are computed and added to the running probability total. In the absence of motion in this space, no new voxels are added and only the initial voxels occupy the space.

G. Instantaneous Probability

In addition to cumulative probability, the instantaneous probability is also provided by the voxel method. The cumulative probability can never be less than the instantaneous, so the maximum instantaneous probability over the time interval should be used as an absolute lower bound. If any of the methods produce a number below this then there is a violation of the assumptions on which the method is based; the relative motion and/or the intermediate tolerances are insufficient to support the computation.

Each method uses a different shape (right cylinder, parallelepipeds, and sphere modeled as small cubes) to represent the collision tube. For proper comparison the effect of these shapes must be accounted for or eliminated at the beginning and end of the time span. One way to address this is to begin and end the time span in a region of very low probability density so that these differences will be inconsequential in the overall calculation and subsequent comparison. If the instantaneous probability is very near zero at these times, then the results can be properly compared.

IV. Conclusion

A simplified Monte Carlo process was employed to assess the satellite collision probability computations of various methods. No assumptions were made regarding the constancy or direction of the relative velocity over the encounter's time span. Two statistical bounding criteria were used to determine the minimum number of cases needed. The Monte Carlo results were compared to probability computations that use the unperturbed orbital data at TCA. No attempt was made to simulate real-world perturbations such as atmospheric drag and/or various gravity fields. Because no unique or complicated force models were used the results can be easily repeated and independently validated.

Three requirements had to be met to equitably compare the results and assure no corresponding assumptions were violated. Because each method uses a different shape (right cylinder, parallelepiped, or sphere represented by small cubes) it was necessary to begin and end the time span in a region of very low probability density so that these differences would be inconsequential in the overall calculation and subsequent comparison. If the change in cumulative probability over time was very near zero at both ends of the time span, then the first requirement was satisfied.

Each method tested had limiting assumptions on which it was based. Gaps, overlaps, and slight misrepresentation of combined object shape in the probability density space all contribute differently to computational error. Preliminary results indicated that the adjoining cylinder method may result in greater than 5% error when the relative velocity is below 0.05 m/s, the parallelepiped method may result in greater than 5% error when the relative velocity is below 0.005 m/s and the voxel method may result in greater than 5% error when the relative velocity is below 0.0005 m/s; these comprise initial estimates regarding the bounds of utility. If the relative velocity for a prescribed method met or exceeded the corresponding minimum, then the second requirement was satisfied.

Lastly, the result of any cumulative method should never be less than the maximum instantaneous probability. If so, then this was an indicator that an assumption had been violated or a limit exceeded. If the cumulative probability for a prescribed method equaled or exceeded the maximum instantaneous probability, then the third requirement was satisfied.

The test cases involved linear and nonlinear relative motion for satellites in geosynchronous orbits (GEO) and low earth orbits (LEO), as well as nonlinear relative motion for highly-eccentric orbits (HEO). Two cases involved no relative motion whatsoever. The tests were designed to showcase differences due to object size variation and to demonstrate the evolution of cumulative probability with respect to various combinations of covariance shape, orientation, and relative motion. In addition, several tests pushed the methods beyond their bounds or assumptions.

V. Acknowledgements

Dr. James Wright is a Senior Advisory Software Developer with Analytical Graphics, Inc. (AGI), and suggested using Herrick's universal variables to rapidly propagate orbital states and covariance. Dr. Vincent Coppola is also an AGI Senior Advisory Software Developer and was instrumental in reviewing the implementation details of the various methods. Dr. Bao Nguyen is a Senior Scientist for the Defence Research and Development Canada (DRDC) Centre of Operational Research and Analysis and recommended investigating Chernoff-Hoeffding bounding as one method to determine the minimum number of Monte Carlo runs for each test case. Dr. David Finkleman is a Senior Scientist with the Center for Space Standards and Innovation and provided guidance and many interim reviews of this paper as did Dr. John Seago, an AGI Astrodynamics Engineer. Mr. Ted Driver is a Senior Navigation Engineer with AGI and assisted in troubleshooting the software implementation of the described methods.

References

- ¹Foster, J. L., and Estes, H. S., "A Parametric Analysis of Orbital Debris Collision Probability and Maneuver Rate for Space Vehicles," NASA/JSC-25898, August 1992.
- ²Chan, K., "Collision Probability Analyses for Earth-Orbiting Satellites," Proceedings of the 7th International Space Conference of Pacific Basin Societies, Nagasaki, Japan, July 1997.
- ³Patera, R. P. "General Method for Calculating Satellite Collision Probability," *Journal of Guidance, Control, and Dynamics*, Vol. 24, No. 4, July-August 2001, pp. 716-722.
- ⁴Chan, K., "Improved Analytical Expressions for Computing Spacecraft Collision Probabilities," AAS Paper No. 03-184, AAS/AIAA Space Flight Mechanics Meeting, Ponce, Puerto Rico, 9-13 February 2003.
- ⁵Chan, K., "Short-Term vs Long-Term Spacecraft Encounters," AIAA Paper No. 2004-5460, AIAA/AAS Astrodynamics Specialist Conference, Providence, Rhode Island, 16-19 August, 2004.
- ⁶Alfano, S. "A Numerical Implementation of Spherical Object Collision Probability," *Journal of the Astronautical Sciences*, Vol. 53, No. 1, January-March 2005, pp. 103-109.
- ⁷Patera, R. P. "Calculating Collision Probability for Arbitrary Space-Vehicle Shapes via Numerical Quadrature," *Journal of Guidance, Control, and Dynamics*, Vol. 28, No. 6, November-December 2005, pp. 1326-1328.
- ⁸Alfano, S., "Review of Conjunction Probability Methods for Short-term Encounters," AAS Paper No. 07-148, AAS/AIAA Space Flight Mechanics Meeting, Sedona, Arizona, 28 January-01 February 2007.
- ⁹Chan, K., "Spacecraft Collision Probability for Long-Term Encounters," AAS Paper No. 03-549, AAS/AIAA Astrodynamics Specialist Conference, Big Sky, Montana, 3-7 August, 2003.
- ¹⁰Patera, R. P. "Satellite Collision Probability for Nonlinear Relative Motion," *Journal of Guidance, Control, and Dynamics*, Vol. 26, No. 5, 2003, pp. 728-733.
- ¹¹Alfano, S., "Addressing Nonlinear Relative Motion For Spacecraft Collision Probability," AIAA Paper No. 2006-6760, 15th AAS/AIAA Astrodynamics Specialist Conference, Keystone, Colorado, Aug 21-24, 2006.
- ¹²McKinley, D. P., "Development of a Nonlinear Probability Collision Tool for the Earth Observing System," AIAA Paper No. 2006-6295, 15th AAS/AIAA Astrodynamics Specialist Conference, Keystone, Colorado, Aug 21-24, 2006.
- ¹³Vallado, D. A., *Fundamentals of Astrodynamics and Applications*, 3rd ed., Microcosm Press, Hawthorne, California, and Springer, New York, New York, 2007, p. 800.
- ¹⁴Alfano, S. "Beta Conjunction Analysis Tool," AAS Paper No. 07-393, AAS/AIAA Astrodynamics Specialist Conference, Mackinac Island, Michigan, 19-23 August, 2007.
- ¹⁵Chao, C-C., and Park, T. H., "A Benchmark Monte Carlo Numerical Verification of Computed Probability of Collision," AIAA Paper No. 2002-4633, AAS/AIAA Astrodynamics Specialist Conference and Exhibit, Monterey, California, Aug 5-8, 2002.
- ¹⁶Alfano, S. "Determining Satellite Close Approaches," *Journal of the Astronautical Sciences*, Vol. 41, No. 2, April-June 1993, pp. 217-225.
- ¹⁷Herrick, S., *Astrodynamics Orbit Correction, Perturbation Theory, Integration*, Volume 2, Van Nostrand Reinhold Company, London, 1972, pp. 37-77.
- ¹⁸Chernoff, H., "A Measure of Asymptotic Efficiency for Tests of a Hypothesis Based On the Sum of Observations," *The Annals of Mathematical Statistics*, 1952, Vol. 23, pp. 493-507.
- ¹⁹Hoeffding, W., "Probability Inequalities for Sums of Bounded Random Variables," *Journal of the American Statistical Association*, Vol. 58, No. 301, March 1963, pp. 13-30.
- ²⁰Dagum, P., Karp, R., Luby, M., and Ross, S, "An Optimal Algorithm for Monte Carlo Estimation," *SIAM Journal on Computing*, Volume 29, Issue 5, March 2000, pp.1484-1496.

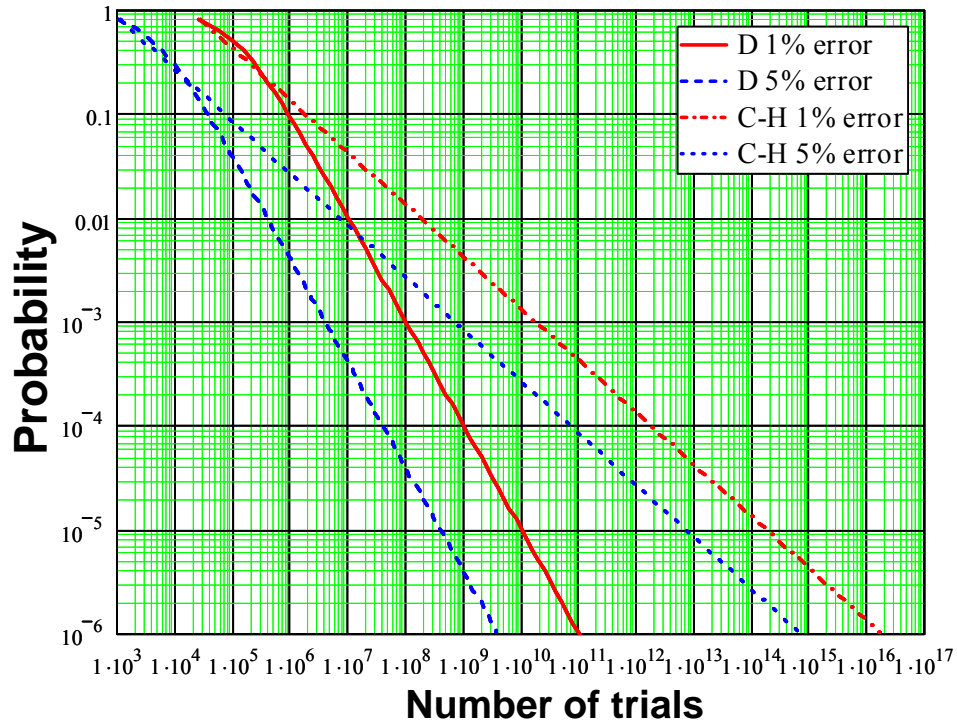


Figure 1. Chernoff-Hoeffding (C-H) versus Dagum (D) Bounding
1% and 5% relative error with 95% confidence.

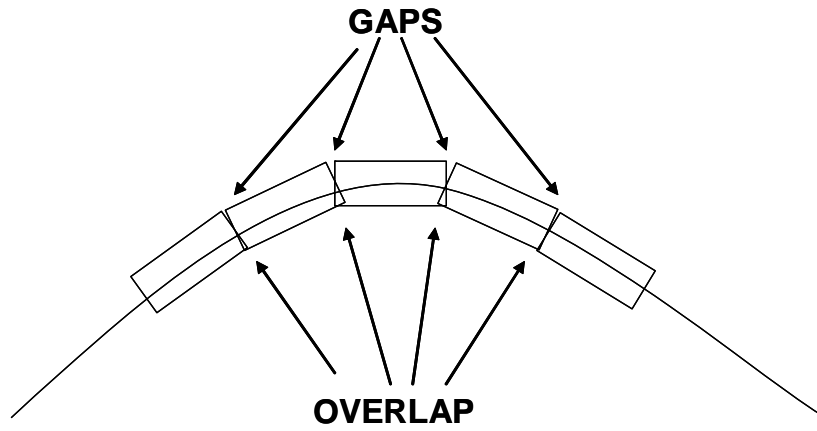


Figure 2. Tube Sections for Nonlinear Relative Motion Track.
Nonlinear motion causes gaps and overlaps where the tube sections meet.

Appendix A – Test cases

Two Monte Carlo simulations were performed for each test case. With the exception of Case 7, the first simulation used one million random combinations and the second used 100 million. The Chernoff-Hoeffding and Dagum bounds were then determined based on the results of the larger simulation. It is inferred that the Monte Carlo result is a reasonable apriori estimate of the true probability if the bound is less than the number of trials in the larger simulation. All but one of the test cases were crafted in such a way to produce Monte Carlo results with probabilities greater than 0.001; this ensured the adequacy of 100 million simulations for 1% error with 95% confidence using the Dagum bound. For Case 7 it was important to simulate one billion random combinations. The probability obtained from the larger simulation was used to reference the results of the various methods tested as well as to examine the difference in results for the lesser simulation.

The Fractional Probability Threshold was set to 0.01 for all cases. If the difference between linear and nonlinear results were above 1%, then it was expected that the minimum velocity computed from the linearity test would exceed the actual minimum velocity at TCA. For convenience, the actual fractional probability was also computed to determine if the threshold was exceeded.

The number of radial or circumferential divisions (n) was set to 50 and 100 for most cases to determine how the answer varies with differing divisions of the combined object. For Case 5 it was necessary to increase this number when using Patera's method in accordance with his recommendations. Only the linear and adjoining right cylinder calculations were effected; for Case 5 only those results were shown with the higher value of n .

Each method has limiting assumptions on which it is based. Gaps, overlaps, and slight misrepresentation of combined object shape in the probability density space all contribute differently to computational error. Preliminary results indicated that the adjoining cylinder method may result in greater than 5% error when the relative velocity is below 0.05 m/s. Because the parallelepiped method reduces the gaps and overlaps of the previous method, the method may result in greater than 5% error when the relative velocity is below 0.005 m/s. Finally, preliminary results showed that the voxel method may result in greater than 5% error when the relative velocity is below 0.0005 m/s.

A Cumulative Probability Chart derived from the voxel method is included for each case to aid in understanding how the probability evolved over the given time span. Typically the along-track uncertainty grows quicker than the other two dimensions and causes an elongation of the positional covariance ellipsoid along the velocity vector. The nonlinear relative motion may cause the conjuncting object to pass through regions of comparable probability density more than once in the time span; this can cause the slope of the cumulative probability curve to change and can even result in intermediate level offs. Because each method uses a different shape (right cylinder, parallelepiped, or sphere represented by small cubes) it is necessary to begin and end the time span in a region of very low probability density so that these differences will be inconsequential in the overall calculation and subsequent comparison. If the change in cumulative probability over time is very near zero at both ends of the time span, then this requirement is satisfied. Equivalently this requirement is satisfied if the instantaneous probability is very near zero at these times. The reader is alerted that although zero instantaneous probability will produce zero slope, the converse is not always true. This is shown in Case 9 where both cumulative and instantaneous probabilities are displayed.

Maximum instantaneous probability over the time span is also provided for each case. The result of any cumulative method should never be less than the maximum instantaneous probability. If so, then this is an indicator that an assumption has been violated or a limit exceeded. This is demonstrated in Case 8 where the adjoining cylinder method produces results below the maximum instantaneous probability.

Position, velocity, and associated covariance data are provided for each case at epoch and also at the Time of Closest Approach. In Cases 11 and 12 there is no relative motion and therefore no closest approach; for those cases the TCA was arbitrarily set to one day after epoch.

Case 1

This case involves nonlinear relative motion for two satellites in geosynchronous orbits (GEO) where the mean miss distance at TCA is less than the combined object radius. There is over a 30% difference between the linear and Monte Carlo results. Based on the Fractional Probability Threshold of 0.01 the relative velocity at TCA is about an order of magnitude below what would be needed to drive the difference between linear and nonlinear results below 1%. Less than 16,000 Monte Carlo runs are needed for the results to be considered statistically significant. As can be seen in the Cumulative Probability Chart, the relative covariance shape and orientation cause the probability to begin accumulating about 2000 seconds prior to TCA, then level off about 2000 seconds after TCA where a volume of low density is entered, then pick up again around 9500 seconds. The slope in the Cumulative Probability Chart is very near zero at both ends of the time span, satisfying the requirement for comparing the various methods. Although the relative velocity is below the suggested adjoining cylinders threshold, those results are within 5% of the large Monte Carlo simulation result.

Method	Conj Prob	diff wrt MC_e8	Other Data	Values
Monte Carlo (10e6)	0.216602000	-0.40%	Chernoff trials (1% error, 95% confidence)	3.92E+05
Monte Carlo (10e8)	0.217467140	0.00%	Dagum trials (1% error, 95% confidence)	1.57E+04
Voxels (n=50)	0.221471977	1.84%	Combined object radius (m)	15
Adjoining Cylinders (n=50)	0.214914675	-1.17%	Fractional Probability Threshold	0.01
Parallelepipeds (n=50)	0.222322909	2.23%	MC_e8 Fractional Probability	0.325188
Linear (Alfano n=50)	0.146749659	-32.52%		
Linear (Patera n=50)	0.146749507	-32.52%	Final Time From TCA (seconds +/-)	21600
Max Instantaneous (n=50)	0.097584783	-55.13%	Final Sigma Limit	3000
Voxels (n=100)	0.217088649	-0.17%	Maximum Time Step (seconds)	10
Adjoining Cylinders (n=100)	0.214759470	-1.25%	Incremental Sigma Limit	1
Parallelepipeds (n=100)	0.222322904	2.23%	Incremental angle limit (degrees)	1
Linear (Alfano n=100)	0.146749549	-32.52%		
Linear (Patera n=100)	0.146749497	-32.52%	Relative Velocity at TCA (m/s)†	0.014142378
Max Instantaneous (n=100)	0.097552603	-55.14%	Minimum Velocity needed (m/s)	0.146569121
			† motion below threshold	

Table A1: Case 1 Parameters and Results

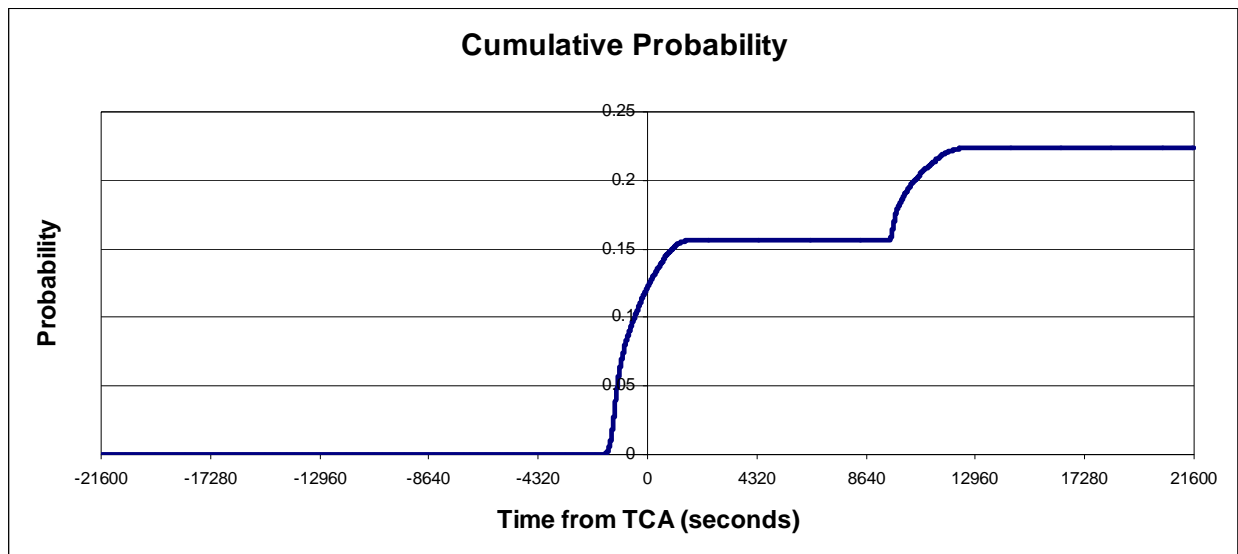


Figure A1: Case 1 Cumulative Probability over Time

Case 2

This case involves nonlinear relative motion for two satellites in geosynchronous orbits (GEO) and is identical in motion and covariance to the previous one but with a smaller combined object radius; the mean miss distance at TCA is greater than the combined object radius. This was done to showcase differences just due to object size variation. There is over a 60% difference between the linear and Monte Carlo results. Based on the Fractional Probability Threshold of 0.01 the relative velocity at TCA is about three times less than what would be needed to drive the difference between linear and nonlinear results below 1%. Over six million Monte Carlo runs are needed for the results to be considered statistically significant. As can be seen in the Cumulative Probability Chart, the relative covariance shape and orientation cause the probability to begin accumulating about 1000 seconds prior to TCA, then level off about 500 seconds after TCA where a volume of low density is entered, then pick up again around 11,000 seconds. The slope in the Cumulative Probability Chart is very near zero at both ends of the time span, satisfying the requirement for comparing the various methods. Although the relative velocity is below the suggested adjoining cylinders threshold, those results are within 5% of the large Monte Carlo simulation result.

Method	Conj Prob	diff wrt MC_e8	Other Data	Values
Monte Carlo (10e6)	0.015546000	-1.21%	Chernoff trials (1% error, 95% confidence)	7.20E+07
Monte Carlo (10e8)	0.015736620	0.00%	Dagum trials (1% error, 95% confidence)	6.52E+06
Voxels (n=50)	0.015823587	0.55%	Combined Object Radius (m)	4
Adjoining Cylinders (n=50)	0.016399941	4.22%	Fractional Probability Threshold	0.01
Parallelepipeds (n=50)	0.016294662	3.55%	MC_e8 Fractional Probability	0.604600
Linear (Alfano n=50)	0.006222269	-60.46%		
Linear (Patera n=50)	0.006222266	-60.46%	Final Time From TCA (seconds +/-)	21600
Max Instantaneous (n=50)	0.006332181	-59.76%	Final Sigma Limit	3000
Voxels (n=100)	0.015549311	-1.19%	Maximum Time Step (seconds)	10
Adjoining Cylinders (n=100)	0.016399941	4.22%	Incremental Sigma Limit	1
Parallelepipeds (n=100)	0.016291997	3.53%	Incremental angle limit (degrees)	1
Linear (Alfano n=100)	0.006222267	-60.46%		
Linear (Patera n=100)	0.006222266	-60.46%	Relative Velocity at TCA (m/s)†	0.01414238
Max Instantaneous (n=100)	0.006325098	-59.81%	Minimum Velocity needed (m/s)	0.034561836
			† motion below threshold	

Table A2: Case 2 Parameters and Results

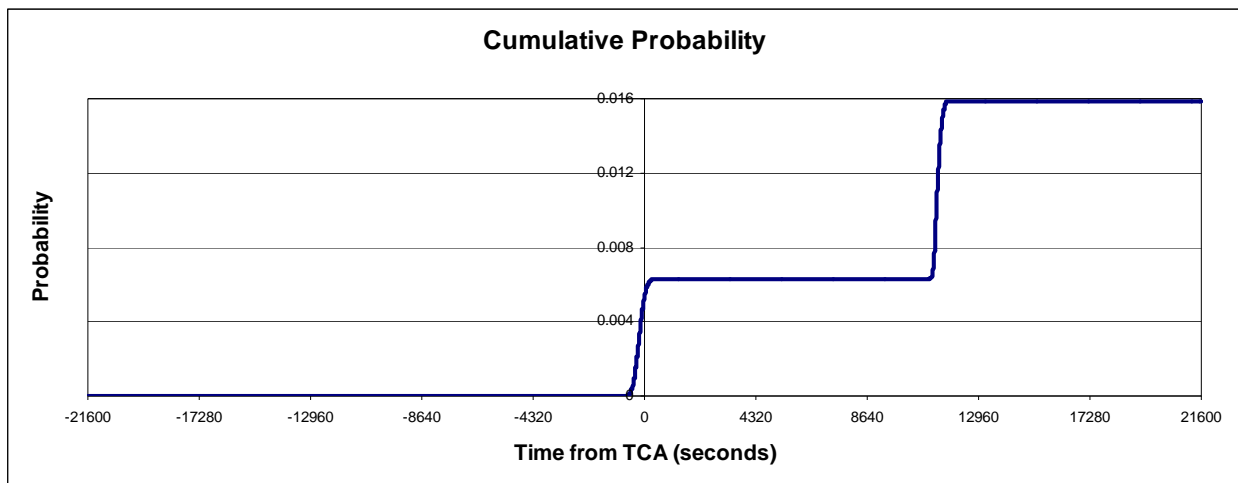


Figure A2: Case 2 Cumulative Probability over Time

Case 2 At Time of Closest Approach (TCA, 280800 seconds after epoch)

Primary Object ECI position (m)	41874155.8717350000	0.0000000000	
Primary Object ECI velocity (m/s)	-11.3735715995	0.0000000000	
Primary Object ECI covariance (meters & seconds)			
	6494.07963584490000000000	-376.1384919642100000000000	0.015989491092283000000000
	-376.1384919642100000000000	22.5594545658280000000000	-0.0098831421764957000000
	0.0000000000000000000000	0.0000000000000000000000	0.0000000000000000000000
	0.015989491092283000000000	-0.0000000000000000000000	0.0000000000000000000000
	-0.494261677654860000000000	0.0285694535838890000000	-0.0000012122347193874000
	0.0000000000000000000000	0.0000000000000000000000	0.0000000000000000000000
Secondary Object ECI position (m)	41874156.3720710000	4.9999660260	
Secondary Object ECI velocity (m/s)	-11.3635714597	-0.0000013581	
Secondary Object ECI covariance (meters & seconds)			
	6494.2249444340000000000000	-376.1560252678700000000000	0.015992179686283000000000
	-376.1560252678700000000000	22.560635191994000000000000	-0.0000000000000000000000
	-0.000044917281068031000000	0.0000255014600181110000	0.0000000000000000000000
	0.015992179686283000000000	-0.0000000000000000000000	0.0000000000000000000000
	-0.494272102084410000000000	0.028570751733036000000000	-0.0000012122347193874000
	-0.0000000000000000000000	0.0000000000000000000000	0.0000000000000000000000

Case 3

This case involves linear relative motion for two satellites in geosynchronous orbits (GEO) where the mean miss distance at TCA is less than the combined object radius. There is little difference between the linear and Monte Carlo results. Based on the Fractional Probability Threshold of 0.01 the relative velocity at TCA is orders of magnitude greater than what would be needed to drive the difference between linear and nonlinear results above 1%. Almost one million Monte Carlo runs are needed for the results to be considered statistically significant. As can be seen in the Cumulative Probability Chart, this brief encounter causes the probability to grow abruptly at TCA due to rapid traversal of the probability density space. As expected for a linear encounter, the slope in the Cumulative Probability Chart is very near zero at both ends of the time span and satisfies the requirement for comparing the various methods.

Method	Conj Prob	diff wrt MC_e8	Other Data	Values
Monte Carlo (10e6)	0.100337000	-0.51%	Chernoff trials (1% error, 95% confidence)	1.84E+06
Monte Carlo (10e8)	0.100846420	0.00%	Dagum trials (1% error, 95% confidence)	9.54E+05
Voxels (n=50)	0.099791893	-1.05%	Combined Object Radius (m)	15
Adjoining Cylinders (n=50)	0.100350598	-0.49%	Fractional Probability Threshold	0.01
Parallelepipeds (n=50)	0.100367848	-0.47%	MC_e8 Fractional Probability	0.004912
Linear (Alfano n=50)	0.100351871	-0.49%		
Linear (Patera n=50)	0.100350890	-0.49%	Final Time From TCA (seconds +/-)	21600
Max Instantaneous (n=50)	0.099791893	-1.05%	Final Sigma Limit	3000
Voxels (n=100)	0.099778793	-1.06%	Maximum Time Step (seconds)	10
Adjoining Cylinders (n=100)	0.100350471	-0.49%	Incremental Sigma Limit	1
Parallelepipeds (n=100)	0.100340544	-0.50%	Incremental angle limit (degrees)	1
Linear (Alfano n=100)	0.100351176	-0.49%		
Linear (Patera n=100)	0.100351018	-0.49%	Relative Velocity at TCA (m/s)	16.0669226
Max Instantaneous (n=100)	0.099778793	-1.06%	Minimum Velocity needed (m/s)	0.007774746

Table A3: Case 3 Parameters and Results

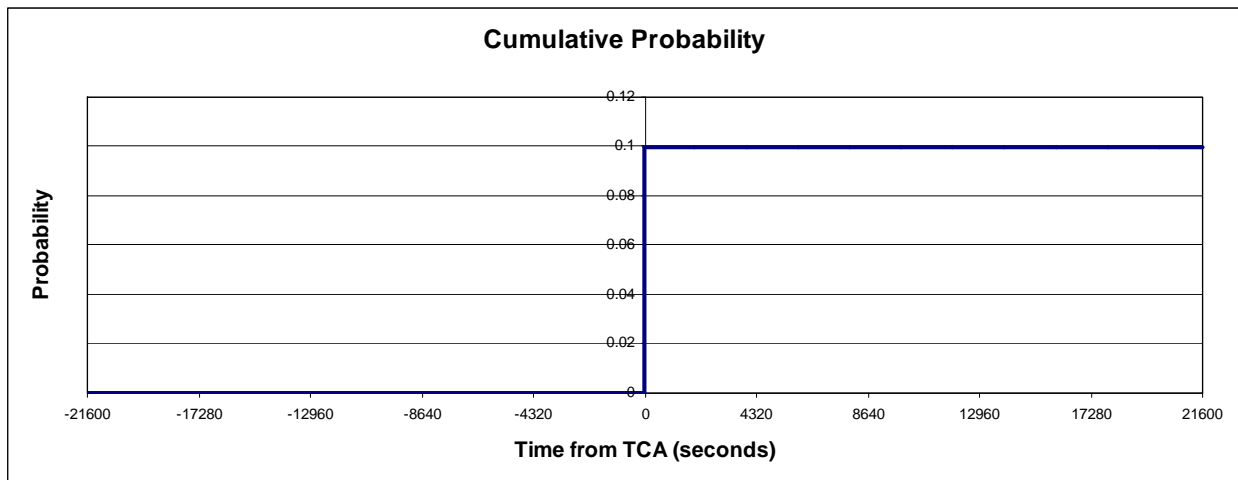


Figure A3: Case 3 Cumulative Probability over Time

Case 4

This case involves nonlinear relative motion for two satellites in geosynchronous orbits (GEO) where the mean miss distance at TCA is greater than the combined object radius. There is over a 30% difference between the linear and Monte Carlo results. Based on the Fractional Probability Threshold of 0.01 the relative velocity at TCA is roughly half what would be needed to drive the difference between linear and nonlinear results below 1%. Over one million Monte Carlo runs are needed for the results to be considered statistically significant. As can be seen in the Cumulative Probability Chart, the relative covariance shape and orientation cause the probability to begin accumulating about 3000 seconds after TCA then level off about 11,000 seconds. The slope in the Cumulative Probability Chart is very near zero at both ends of the time span, satisfying the requirement for comparing the various methods. This example demonstrates that probability does not always accumulate around the time of closest approach due to certain combinations of relative motion and covariance shape. It also shows how the gaps and overlaps in the adjoining right cylinders can cause large errors and how those errors are reduced by the Parallelepiped and Voxel methods. This indicates that the adjoining cylinder method may result in greater than 5% error when the relative velocity is below 0.05 m/s.

Method	Conj Prob	diff wrt MC_e8	Other Data	Values
Monte Carlo (10e6)	0.078974000	8.05%	Chernoff trials (1% error, 95% confidence)	2.96E+06
Monte Carlo (10e8)	0.073089530	0.00%	Dagum trials (1% error, 95% confidence)	1.24E+06
Voxels (n=50)	0.072577999	-0.70%	Combined Object Radius (m)	15
Adjoining Cylinders (n=50)	0.024146760	-66.96%	Fractional Probability Threshold	0.01
Parallelepipeds (n=50)	0.071779248	-1.79%	MC_e8 Fractional Probability	0.318272
Linear (Alfano n=50)	0.049354780	-32.47%		
Linear (Patera n=50)	0.049800817	-31.86%	Final Time From TCA (seconds +/-)	21600
Max Instantaneous (n=50)	0.034202499	-53.20%	Final Sigma Limit	3000
Voxels (n=100)	0.073900169	1.11%	Maximum Time Step (seconds)	10
Adjoining Cylinders (n=100)	0.024149456	-66.96%	Incremental Sigma Limit	1
Parallelepipeds (n=100)	0.071653864	-1.96%		
Linear (Alfano n=100)	0.049323406	-32.52%	Incremental angle limit (degrees)	1
Linear (Patera n=100)	0.049827212	-31.83%	Relative Velocity at TCA (m/s)†	0.01903342
Max Instantaneous (n=100)	0.034196773	-53.21%	Minimum Velocity needed (m/s)	0.03473549
			† motion below threshold	

Table A4: Case 4 Parameters and Results

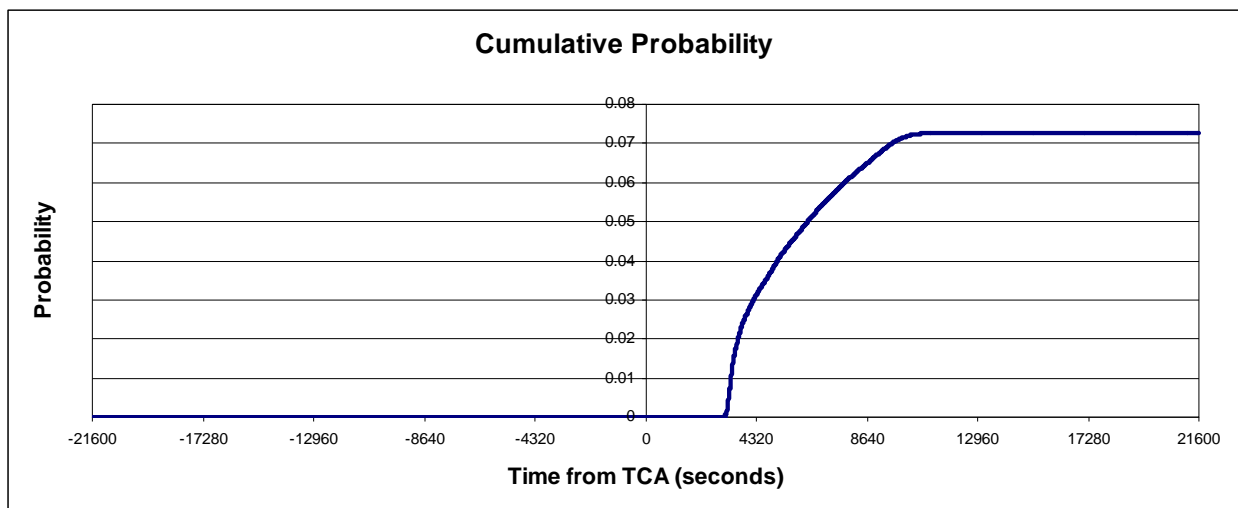


Figure A4: Case 4 Cumulative Probability over Time

Case 4 At Epoch

Primary Object ECI position (m)

-30285329.8697380000 -27707671.2985530000 0.0000000000

Primary Object ECI velocity (m/s)

-2131.9561967731 2289.9864650781 0.0000000000

Primary Object ECI covariance (meters & seconds)

0.0632153919251120000000 -0.0249362221280420000000 0.00000000000000000000 0.00000000000000000000 0.00000000000000000000 0.00000000000000000000
-0.0249362221280420000000 0.0667946080748880000000 0.00000000000000000000 0.00000000000000000000 0.00000000000000000000 0.00000000000000000000
0.00000000000000000000 0.00000000000000000000 0.04000000000000000000 0.00000000000000000000 0.00000000000000000000 0.00000000000000000000
0.00000000000000000000 0.00000000000000000000 0.00000000000000000000 0.0000000100000000000000 0.00000000000000000000 0.00000000000000000000
0.00000000000000000000 0.00000000000000000000 0.00000000000000000000 0.00000000000000000000 0.00000001000000000000 0.00000000000000000000
0.00000000000000000000 0.00000000000000000000 0.00000000000000000000 0.00000000000000000000 0.00000000000000000000 0.0000000100000000000000

Secondary Object ECI position (m)

-30289645.6519680000 -27703079.3787730000 -3.5557323237

Secondary Object ECI velocity (m/s)

-2131.6028955093 2290.3175429528 0.0002668288

Secondary Object ECI covariance (meters & seconds)

0.0632076742116520000000 -0.0249356685947740000000 -0.0000000029050800127257 0.00000000000000000000 0.00000000000000000000 0.00000000000000000000
-0.0249356685947740000000 0.0667923257883480000000 0.0000000031213861319314 0.00000000000000000000 0.00000000000000000000 0.00000000000000000000
-0.0000000029050800127257 0.0000000031213861319314 0.04000000000000000000 0.00000000000000000000 0.00000000000000000000 0.00000000000000000000
0.00000000000000000000 0.00000000000000000000 0.00000000000000000000 0.00000001000000000000 0.00000000000000000000 0.00000000000000000000
0.00000000000000000000 0.00000000000000000000 0.00000000000000000000 0.00000000000000000000 0.00000001000000000000 0.00000000000000000000
0.00000000000000000000 0.00000000000000000000 0.00000000000000000000 0.00000000000000000000 0.00000000000000000000 0.0000000100000000000000

Case 4 At Time of Closest Approach (TCA, 250560 seconds after epoch)

Primary Object ECI position (m)	-28570333.4483850000	-29444167.1919470000	0.0000000000
Primary Object ECI velocity (m/s)	-2264.3786988144	2161.3955655441	0.0000000000
Primary Object ECI covariance (meters & seconds)	3149.7395861594000000000000	-3009.1218002121000000000000	0.00000000000000000000
	-3009.1218002121000000000000	2874.8685578726000000000000	0.00000000000000000000
	0.000000000000000000000000	0.000000000000000000000000	0.00000000000000000000
	-0.233026440621630000000000	0.000017244984336726000000	0.0000171839238856060000
	-0.232206205394740000000000	0.000017183923885606000000	0.0000171235489169690000
	0.000000000000000000000000	0.000000000000000000000000	0.0000000000000000000000
	-0.000000000000000000000000	-0.0000076019546328751000	0.0000000000000000000000
Secondary Object ECI position (m)	-28570452.2619860000	-29444104.4635150000	-3.7579884938
Secondary Object ECI velocity (m/s)	-2264.3698138968	2161.4123960717	0.0002503315
Secondary Object ECI covariance (meters & seconds)	3149.8133559411000000000000	-3009.2292261314000000000000	-0.0003485408072712500000
	-3009.2292261314000000000000	2875.0065497795000000000000	0.0003329892763827800000
	-0.000348540807271250000000	0.000332989276382780000000	0.000000257850743461980
	-0.233031901362900000000000	0.000017245388624804000000	0.0000171842319033550000
	-0.232210385872320000000000	0.000017184231903355000000	0.0000171237615483970000
	-0.0000000296824042418720	0.0000000283583393524670	-0.000000009965797275807

Case 5

This case involves linear relative motion for two satellites in low earth orbits (LEO) where the mean miss distance at TCA is less than the combined object radius. Because the combined object footprint spans more than one-tenth sigma in the probability density space, Patera's algorithm recommends 360 circumferential divisions for this case. Doing so greatly improves the accuracy of his method as seen in the linear and adjoining cylinder results for n=360. Also, the result of any method should never be less than the maximum instantaneous probability. If so, then this is an indicator that an assumption has been violated or a limit exceeded as is apparent from the linear result for n=50. Based on the Fractional Probability Threshold of 0.01 the relative velocity at TCA is about three times greater than what would be needed to drive the difference between linear and nonlinear results above 1%. Over two million Monte Carlo runs are needed for the results to be considered statistically significant. As can be seen in the Cumulative Probability Chart, this brief encounter causes the probability to quickly grow just prior to TCA with the combined object traversing a significant portion of the probability density space in about 20 seconds. As expected for a linear relative motion encounter, the slope in the Cumulative Probability Chart is very near zero at both ends of the time span and satisfies the requirement for comparing the various methods.

Method	Conj Prob	diff wrt MC_e8	Other Data	Values
Monte Carlo (10e6)	0.044336000	-0.37%	Chernoff trials (1% error, 95% confidence)	9.53E+06
Monte Carlo (10e8)	0.044498913	0.00%	Dagum trials (1% error, 95% confidence)	2.30E+06
Voxels (n=50)	0.044556938	0.13%	Combined Object Radius (m)	10
Adjoining Cylinders (n=50)**	0.052917447	18.92%	Fractional Probability Threshold	0.01
Parallelepipedes (n=50)	0.044658117	0.36%	MC_e8 Fractional Probability	0.003471
Linear (Alfano n=50)	0.044547269	0.11%		
Linear (Patera n=50)**	0.036571416	-17.82%	Final Time From TCA (seconds +/-)	1419
Max Instantaneous (n=50)	0.044547107	0.11%	Final Sigma Limit	3000
Voxels (n=100)	0.044487846	-0.02%	Maximum Time Step (seconds)	1
Adjoining Cylinders (n=100)**	0.044853439	0.80%	Incremental Sigma Limit	1
Parallelepipedes (n=100)	0.044473748	-0.06%	Incremental angle limit (degrees)	1
Linear (Alfano n=100)	0.044487386	-0.03%		
Linear (Patera n=100)**	0.044653357	0.35%	Relative Velocity at TCA (m/s)	0.51962236
Max Instantaneous (n=100)	0.044443994	-0.12%	Minimum Velocity needed (m/s)	0.14490341
**Patera recommends n=360				
Linear (Patera n=360)	0.044492344	-0.01%		
Adjoining Cylinders (n=360)	0.044694997	0.44%		

Table A5: Case 5 Parameters and Results

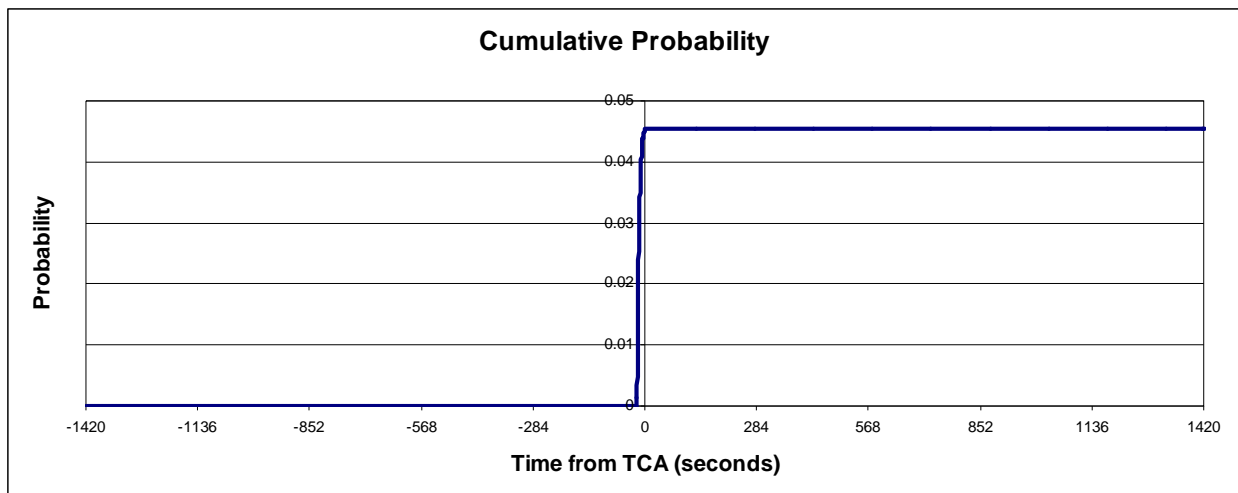


Figure A5: Case 5 Cumulative Probability over Time

Case 5 At Epoch

Primary Object ECI position (m)

-6384206.8367291000 -1809788.8923854000 -1809788.8923854000

Primary Object ECI velocity (m/s)

2832.7325382671 -4996.3701601034 -4996.3701601034

Primary Object ECI covariance (meters & seconds)

0.0469233166114590000000 -0.0122113373074050000000 -0.0122113373074050000000 0.000000000000000000 0.000000000000000000 0.000000000000000000
-0.0122113373074050000000 0.0865383416942710000000 -0.0034616583057294000000 0.000000000000000000 0.000000000000000000 0.000000000000000000
-0.0122113373074050000000 -0.0034616583057294000000 0.0865383416942710000000 0.000000000000000000 0.000000000000000000 0.000000000000000000
0.00000000000000000000 0.00000000000000000000 0.00000000000000000000 0.000000000000000000 0.000000000000000000 0.000000000000000000
0.00000000000000000000 0.00000000000000000000 0.00000000000000000000 0.000000000000000000 0.000000000000000000 0.000000000000000000
0.00000000000000000000 0.00000000000000000000 0.00000000000000000000 0.000000000000000000 0.000000000000000000 0.000000000000000000

Secondary Object ECI position (m)

-6384500.2941289000 -1809180.3432640000 -1808975.9125458000

Secondary Object ECI velocity (m/s)

2831.9641937123 -4996.9514349091 -4996.3957233165

Secondary Object ECI covariance (meters & seconds)

0.0469193569932670000000 -0.0122090956550650000000 -0.0122077160742110000000 0.000000000000000000 0.000000000000000000 0.000000000000000000
-0.0122090956550650000000 0.0865399305509150000000 -0.0034596784745420000000 0.000000000000000000 0.000000000000000000 0.000000000000000000
-0.0122077160742110000000 -0.0034596784745420000000 0.0865407124558180000000 0.000000000000000000 0.000000000000000000 0.000000000000000000
0.00000000000000000000 0.00000000000000000000 0.00000000000000000000 0.000000000000000000 0.000000000000000000 0.000000000000000000
0.00000000000000000000 0.00000000000000000000 0.00000000000000000000 0.000000000000000000 0.000000000000000000 0.000000000000000000
0.00000000000000000000 0.00000000000000000000 0.00000000000000000000 0.000000000000000000 0.000000000000000000 0.000000000000000000

Case 5 At Time of Closest Approach (TCA, 172800 seconds after epoch)

Primary Object ECI position (m)	6878090.1622937000	-17948.6785967000	-17948.6785967000
Primary Object ECI velocity (m/s)	28.0937771808	5382.8902061517	5382.8902061517
Primary Object ECI covariance (meters & seconds)	0.0642045263632400000000	-18.9906919383670000000000	-18.9906919383670000000000
	-18.9906919383670000000000	7904.0447002725000000000000	7903.9662413044000000000000
	-18.9906919383670000000000	7903.9662413044000000000000	7904.0447002725000000000000
	0.029712221972673000000000	-12.380432521341000000000000	0.019392185895765000000000
	-0.000168798797798630000000	0.064200212052864000000000	-0.0001005086487127700000
	-0.000168798797798630000000	0.064168687514337000000000	-0.0001005086487127700000
Secondary Object ECI position (m)	6878089.1619754000	-17946.6789294160	-17947.6782860120
Secondary Object ECI velocity (m/s)	28.3937813158	5383.1902163515	5382.5902081838
Secondary Object ECI covariance (meters & seconds)	0.0621123489818220000000	-18.5520697693830000000000	-18.5500019988590000000000
	-18.5520697693830000000000	7905.3548684174000000000000	7904.3963083026000000000000
	-18.5500019988590000000000	7904.3963083026000000000000	7905.3548684174000000000000
	0.029023568403742000000000	-12.381795445702000000000000	0.019393241165813000000000
	-0.0001652233063971100000	0.064205601367087000000000	-0.0001005114994681300000
	-0.0001652233063971100000	0.064172326730475000000000	-0.0001005114994681300000

Case 6

This case approaches the boundary of linear relative motion for two satellites in low earth orbits (LEO) where the mean miss distance at TCA is less than the combined object radius. Based on the Fractional Probability Threshold of 0.01 the relative velocity at TCA is less than 1.5% above what would be needed to drive the difference between linear and nonlinear results above 1%. About 25 million Monte Carlo runs are needed for the results to be considered statistically significant. The Cumulative Probability Chart shows the probability growing over a span of about 100 seconds very near TCA. The slope at both ends of Cumulative Probability Chart is zero thereby satisfying the requirement for comparing the various methods.

Method	Conj Prob	diff wrt MC_e8	Other Data	Values
Monte Carlo (10e6)	0.004447000	3.41%	Chernoff trials (1% error, 95% confidence)	9.98E+08
Monte Carlo (10e8)	0.004300500	0.00%	Dagum trials (1% error, 95% confidence)	2.45E+07
Voxels (n=50)	0.004349564	1.14%	Combined Object Radius (m)	10
Adjoining Cylinders (n=50)	0.004265579	-0.81%	Fractional Probability Threshold	0.01
Parallelepipeds (n=50)	0.004336181	0.83%	MC_e8 Fractional Probability	0.008128
Linear (Alfano n=50)	0.004335448	0.81%		
Linear (Patera n=50)	0.004335454	0.81%	Final Time From TCA (seconds +/-)	1419
Max Instantaneous (n=50)	0.004187935	-2.62%	Final Sigma Limit	3000
Voxels (n=100)	0.004335323	0.81%	Maximum Time Step (seconds)	1
Adjoining Cylinders (n=100)	0.004265579	-0.81%	Incremental Sigma Limit	1
Parallelepipeds (n=100)	0.004333643	0.77%	Incremental angle limit (degrees)	1
Linear (Alfano n=100)	0.004335455	0.81%		
Linear (Patera n=100)	0.004335454	0.81%	Relative Velocity at TCA (m/s)	0.17322654
Max Instantaneous (n=100)	0.004186446	-2.65%	Minimum Velocity needed (m/s)	0.17114378

Table A6: Case 6 Parameters and Results

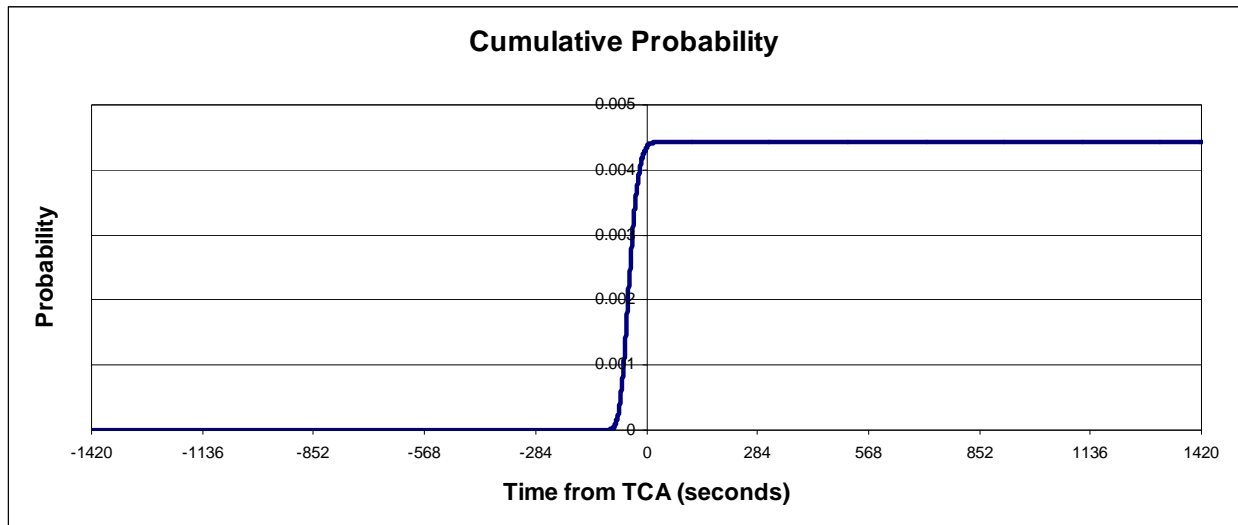


Figure A6: Case 6 Cumulative Probability over Time

Case 6 At Time of Closest Approach (TCA, 172800 seconds after epoch)

Primary Object ECI position (m)	6877715.6342470000	53834.2140394360	53834.2140394360	
Primary Object ECI velocity (m/s)	-84.2628278054	5382.5970952289	5382.5970952289	
Primary Object ECI covariance (meters & seconds)	430.0282793977700000000000 -18393.8913813850000000000000 -18393.8913813850000000000000 28.8117756148510000000000 0.1498549485908200000000 0.1498549485908200000000	-18393.8913813850000000000000 790186.9676547000000000000000 790190.5186786500000000000000 -1237.8765173077000000000000 -6.5012185382348000000000 -6.5024449244912000000000	-18393.8913813850000000000000 790186.9676547000000000000000 790190.5186786500000000000000 -1237.8765173077000000000000 -6.5012185382348000000000 -6.5024449244912000000000	28.8117756148510000000000 -1237.87651730770000000000 -1237.87651730770000000000 1.9392157223809000000000 0.0101882182070030000000 0.0000554746815486410000 0.0000539246995341120000
Secondary Object ECI position (m)	6877716.6344015000	53835.2141405120	53836.2137729820	
Secondary Object ECI velocity (m/s)	-84.1628151363	5382.6970892007	5382.4970647006	
Secondary Object ECI covariance (meters & seconds)	429.3528457262700000000000 -18379.89535348700000000000 -18379.21228433200000000000 28.78930421662000000000 0.14973961436546000000 0.1497466073068700000000	-18379.8953534870000000000000 790234.9389582100000000000000 790202.0196828900000000000000 -1237.9226383171000000000000 -6.5015746157359000000000 -6.503099931720880000000000	-18379.2122843320000000000000 790202.0196828900000000000000 790176.2037772900000000000000 -1237.8766321984000000000000 -6.5025593138425000000000 -6.501163126951970000000000	28.7893042166200000000000 -1237.92263831710000000000 -1237.87663219840000000000 1.9392512139259000000000 0.0101885828614530000000 0.0000554774313588150000 0.0000539299529638100000

Case 7

This case involves nonlinear relative motion for two satellites in low earth orbits (LEO) where the mean miss distance at TCA is less than the combined object radius and the cumulative probability is less than 0.001. This was done to test the methods at a lower probability that would require a much greater number of Monte Carlo simulations. At least 662 million Monte Carlo runs are needed for the results to be considered statistically significant. If one is willing to accept a 5% percent error with 95% confidence then 27 million Monte Carlo runs will suffice. Based on the Fractional Probability Threshold of 0.01 the relative velocity at TCA is about nine times smaller than what would be needed to drive the difference between linear and nonlinear results below 1%. The Cumulative Probability Chart shows the probability growing over a span of about 300 seconds around TCA. The slope at both ends of Cumulative Probability Chart is zero thereby satisfying the requirement for comparing the various methods.

Method	Conj Prob	diff wrt MC_e9	Other Data	Values
Monte Carlo (10e6)	0.000151000	-6.48%	Chernoff trials (1% error, 95% confidence)	7.21E+11
Monte Carlo (10e9)	0.000161462	0.00%	Dagum trials (1% error, 95% confidence)	6.62E+08
Voxels (n=50)	0.000164414	1.83%	Combined Object Radius (m)	10
Adjoining Cylinders (n=50)	0.000161677	0.13%	Fractional Probability Threshold	0.01
Parallelepipeds (n=50)	0.000161761	0.18%	MC_e8 Fractional Probability	0.020534
Linear (Alfano n=50)	0.000158147	-2.05%		
Linear (Patera n=50)	0.000158146	-2.05%	Final Time From TCA (seconds +/-)	1419
Max Instantaneous (n=50)	0.000088052	-45.47%	Final Sigma Limit	3000
Voxels (n=100)	0.000161719	0.16%	Maximum Time Step (seconds)	1
Adjoining Cylinders (n=100)	0.000161677	0.13%	Incremental Sigma Limit	1
Parallelepipeds (n=100)	0.000161701	0.15%	Incremental angle limit (degrees)	1
Linear (Alfano n=100)	0.000158147	-2.05%		
Linear (Patera n=100)	0.000158146	-2.05%	Relative Velocity at TCA (m/s)	0.19628974
Max Instantaneous (n=100)	0.000088002	-45.50%	Minimum Velocity needed (m/s)	1.73630872

Table A7: Case 7 Parameters and Results

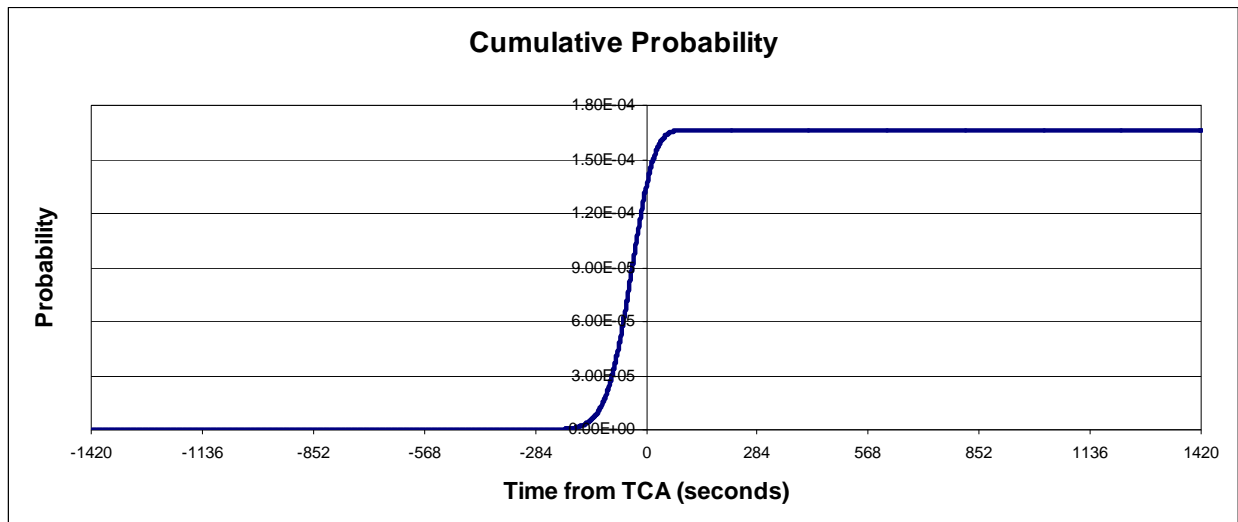


Figure A7: Case 7 Cumulative Probability over Time

Case 7 At Epoch

Primary Object ECI position (m)

1889309.8033002000 1889309.8033002000

Primary Object ECI velocity (m/s)

4960.1786006789 4960.1786006789

Primary Object ECI covariance (meters & seconds)

340.997384637050000000000000 98.9664437757300000000000 98.9664437757300000000000 0.000000000000000000 0.000000000000000000 0.000000000000000000
98.9664437757300000000000 -165.9986923185200000000000 -165.9986923185200000000000 0.000000000000000000 0.000000000000000000 0.000000000000000000
98.9664437757300000000000 -234.0013076814800000000000 234.0013076814800000000000 0.000000000000000000 0.000000000000000000 0.000000000000000000
0.00000000000000000000 0.000000000000000000 0.000000000000000000 0.000000000000000000 0.000000000000000000 0.000000000000000000
0.00000000000000000000 0.000000000000000000 0.000000000000000000 0.000000000000000000 0.000000000000000000 0.000000000000000000
0.00000000000000000000 0.000000000000000000 0.000000000000000000 0.000000000000000000 0.000000000000000000 0.000000000000000000

Secondary Object ECI position (m)

1888217.7447937000 1888150.3615517000

Secondary Object ECI velocity (m/s)

4960.8101452466 4960.6245630827

Secondary Object ECI covariance (meters & seconds)

341.0728283379100000000000 98.9125384111590000000000 98.9125384111590000000000 0.000000000000000000 0.000000000000000000 0.000000000000000000
98.9125384111590000000000 -166.0364140527700000000000 -166.0364140527700000000000 0.000000000000000000 0.000000000000000000 0.000000000000000000
98.9125384111590000000000 -233.9697973112000000000000 233.9697973112000000000000 0.000000000000000000 0.000000000000000000 0.000000000000000000
0.00000000000000000000 0.000000000000000000 0.000000000000000000 0.000000000000000000 0.000000000000000000 0.000000000000000000
0.00000000000000000000 0.000000000000000000 0.000000000000000000 0.000000000000000000 0.000000000000000000 0.000000000000000000
0.00000000000000000000 0.000000000000000000 0.000000000000000000 0.000000000000000000 0.000000000000000000 0.000000000000000000

Case 7 At Time of Closest Approach (TCA, 172800 seconds after epoch)

Primary Object ECI position (m)	-6877469.1698240000	-67773.1837999100	-67773.1837999100	-5382.4047050208	-67773.1837999100	-5382.4047050208	20.73933344231610000000000000	20.73933344231610000000000000
Primary Object ECI velocity (m/s)	106.0806288716	-5382.4047050208	-5382.4047050208	-5382.4047050208	-5382.4047050208	-5382.4047050208	2775.852822122800000000000000	2775.852822122800000000000000
Primary Object ECI covariance (meters & seconds)	47752.9310021520000000000000	-1772101.1180686000000000000000	-1772101.1180686000000000000000	-1772101.1180686000000000000000	-1772101.1180686000000000000000	-1772101.1180686000000000000000	2775.852822122800000000000000	2775.852822122800000000000000
	-1772101.1180686000000000000000	65779308.8829140000000000000000	65779308.8829140000000000000000	65779308.8829140000000000000000	65779308.8829140000000000000000	65779308.8829140000000000000000	-103038.887088430000000000000000	-103038.887088430000000000000000
	-1772101.1180686000000000000000	65778953.7925150000000000000000	65778953.7925150000000000000000	65778953.7925150000000000000000	65778953.7925150000000000000000	65778953.7925150000000000000000	-103038.887088430000000000000000	-103038.887088430000000000000000
	2775.85282212280000000000000000	-103038.8870884300000000000000	-103038.8870884300000000000000	-103038.8870884300000000000000	-103038.8870884300000000000000	-103038.8870884300000000000000	161.40405348647000000000000000	161.40405348647000000000000000
	20.73933344231610000000000000	-770.141052537920000000000000	-770.141052537920000000000000	-770.141052537920000000000000	-770.141052537920000000000000	-770.141052537920000000000000	1.20650061517550000000000000	1.20650061517550000000000000
	20.73933344231610000000000000	-770.263704454190000000000000	-770.263704454190000000000000	-770.263704454190000000000000	-770.263704454190000000000000	-770.263704454190000000000000	1.20650061517550000000000000	1.20650061517550000000000000
Secondary Object ECI position (m)	-6877468.6856734000	-67775.1550967940	-67775.1550967940	-67775.6360351300	-67775.6360351300	-67775.6360351300	2778.431719458300000000000000	2778.431719458300000000000000
Secondary Object ECI velocity (m/s)	106.2166300696	-5382.5006947728	-5382.5006947728	-5382.3006891309	-5382.3006891309	-5382.3006891309	2778.431719458300000000000000	2778.431719458300000000000000
Secondary Object ECI covariance (meters & seconds)	47842.5562503340000000000000	-1773779.5298260000000000000000	-1773779.5298260000000000000000	-1773779.5298260000000000000000	-1773779.5298260000000000000000	-1773779.5298260000000000000000	2778.431719458300000000000000	2778.431719458300000000000000
	-1773779.5298260000000000000000	65780452.9316690000000000000000	65780452.9316690000000000000000	65777653.2864190000000000000000	65777653.2864190000000000000000	65777653.2864190000000000000000	-103038.815512370000000000000000	-103038.815512370000000000000000
	-1773779.5298260000000000000000	65777653.2864190000000000000000	65777653.2864190000000000000000	65775564.0283980000000000000000	65775564.0283980000000000000000	65775564.0283980000000000000000	161.40102219608000000000000000	161.40102219608000000000000000
	2778.43171945830000000000000000	-103038.8155123700000000000000	-103038.8155123700000000000000	-103038.8155123700000000000000	-103038.8155123700000000000000	-103038.8155123700000000000000	1.20649734149760000000000000	1.20649734149760000000000000
	20.75895991149200000000000000	-770.152944594630000000000000	-770.152944594630000000000000	-770.152944594630000000000000	-770.152944594630000000000000	-770.152944594630000000000000	0.009104007846558300000000	0.009104007846558300000000
	20.75940014264500000000000000	-770.291830807860000000000000	-770.291830807860000000000000	-770.140631576590000000000000	-770.140631576590000000000000	-770.140631576590000000000000	0.008948995228248100000000	0.008948995228248100000000

Case 8

This case involves nonlinear relative motion for two satellites in mid-earth orbits (MEO) where the mean miss distance at TCA is less than the combined object radius. This is an especially stressing case due a tight turn in the relative trajectory coupled with very low relative velocity. The relative velocity is below the recommended threshold for the adjoining cylinders and parallelepipeds but not for the voxels. The gaps and overlaps in the probability space are significant enough to diminish the results of the adjoining cylinders method by almost 16%, leading to a cumulative probability that is below the maximum instantaneous probability. The parallelepiped method experiences smaller gaps and overlaps resulting in less than 5% difference. The voxel method is best able to handle the turn and produces results that are within 1% of the Monte Carlo results. Over 3 million Monte Carlo runs are needed for the results to be considered statistically significant. Based on the Fractional Probability Threshold of 0.01 the relative velocity at TCA is about two orders of magnitude below what would be needed to drive the difference between linear and nonlinear results below 1%. The Cumulative Probability Chart shows the probability growing over a span of about 10,000 seconds with much of the accumulation occurring prior to TCA. The slope at both ends of Cumulative Probability Chart is zero thereby satisfying the requirement for comparing the various methods.

Method	Conj Prob	diff wrt MC_e8	Other Data	Values
Monte Carlo (10e6)	0.033806000	-4.11%	Chernoff trials (1% error, 95% confidence)	1.70E+07
Monte Carlo (10e8)	0.035256080	0.00%	Dagum trials (1% error, 95% confidence)	3.11E+06
Voxels (n=50)	0.034984976	-0.77%	Combined Object Radius (m)	4
Adjoining Cylinders (n=50) *	0.029623874	-15.98%	Fractional Probability Threshold	0.01
Parallelepipeds (n=50)	0.033625371	-4.63%	MC_e8 Fractional Probability	0.047989
Linear (Alfano n=50)	0.036948070	4.80%		
Linear (Patera n=50)	0.036947992	4.80%	Final Time From TCA (seconds +/-)	10135
Max Instantaneous (n=50)	0.032324594	-8.31%	Final Sigma Limit	3000
Voxels (n=100)	0.035133761	-0.35%	Maximum Time Step (seconds)	5
Adjoining Cylinders (n=100) *	0.029623874	-15.98%	Incremental Sigma Limit	1
Parallelepipeds (n=100)	0.033628687	-4.62%	Incremental angle limit (degrees)	1
Linear (Alfano n=100)	0.036948008	4.80%		
Linear (Patera n=100)	0.036947992	4.80%	Relative Velocity at TCA (m/s)†	0.000898468
Max Instantaneous (n=100)	0.032313871	-8.35%	Minimum Velocity needed (m/s)	0.098259791
* Prob < max instantaneous			† motion below threshold	

Table A8: Case 8 Parameters and Results

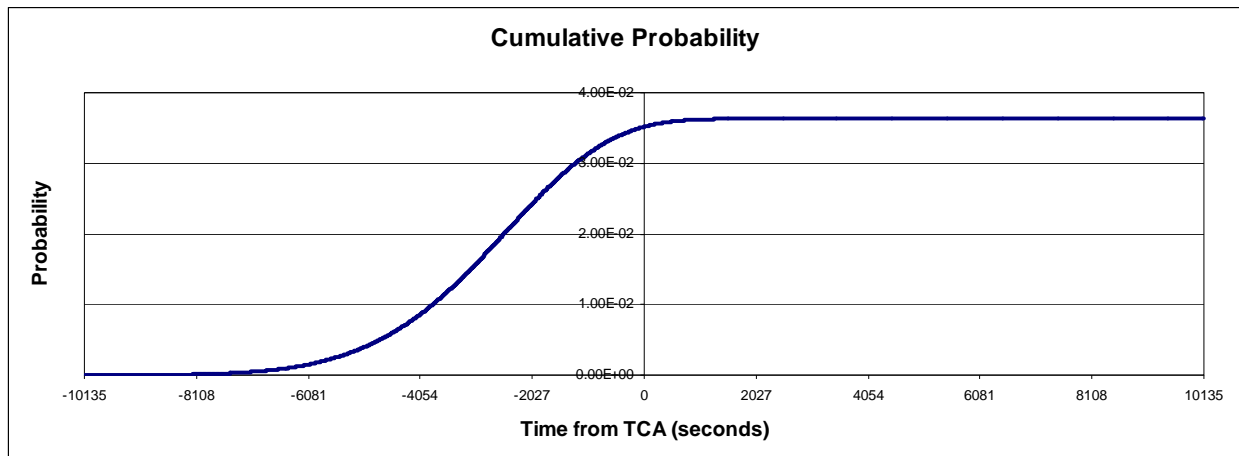


Figure A8: Case 8 Cumulative Probability over Time

Case 8 At Time of Closest Approach (TCA, 172800 seconds after epoch)

Primary Object ECI position (m)	14971649.316903000	-20270398.211949000	4076385.1140421000				
Primary Object ECI velocity (m/s)	1012.2565120970	1460.8114696427	3527.3938005475				
Primary Object ECI covariance (meters & seconds)	153.4102988009900000000000	250.6060960119400000000000	567.3820317872500000000000	-0.0590788814627830000000	0.0810431674389880000000		
	250.6060960119400000000000	411.0105879758300000000000	929.4901965968200000000000	-0.0967388981287660000000	0.1328002384799800000000		
	567.3820317872500000000000	929.4901965968200000000000	2104.6873950138000000000000	-0.2190487405344600000000	0.3006128540761800000000		
	-0.059078881462783000000000	-0.096738898128766000000000	-0.2190487405344600000000	0.0000228004568718450000	-0.0000312870039593820000		
	0.081043167438988000000000	0.132800238479980000000000	0.3006128540761800000000	-0.0000312870039593820000	0.0000429406476039980000		
	-0.014865617039894000000000	-0.024239891541315000000000	-0.055007273173277000000000	0.0000057271493246217000	-0.0000078529855374707000		
Secondary Object ECI position (m)	14971649.362587000	-20270399.371468000	4076387.8292675000				
Secondary Object ECI velocity (m/s)	1012.2574006063	1460.8115969929	3527.3938402543				
Secondary Object ECI covariance (meters & seconds)	153.4108490343700000000000	250.6064883119600000000000	567.3832041704800000000000	-0.0590789976978420000000	0.0810433141358050000000		
	250.6064883119600000000000	411.0104033221400000000000	929.4902378303400000000000	-0.0967388939076360000000	0.1328002113806000000000		
	567.3832041704800000000000	929.4902378303400000000000	2104.6885373437000000000000	-0.2190488400577000000000	0.3006129406437300000000		
	-0.059078997697842000000000	-0.096738893907636000000000	-0.2190488400577000000000	0.0000228004651384930000	-0.0000312870101971610000		
	0.081043314135805000000000	0.132800211380600000000000	0.3006129406437300000000	-0.0000312870101971610000	0.0000429406491462000000		
	-0.014865678390079000000000	-0.024239942513815000000000	-0.055007415866958000000000	0.0000057271636219629000	-0.0000078530038400398000		

Case 9

This case involves nonlinear relative motion for two satellites in highly-eccentric orbits (HEO) where the mean miss distance at TCA is greater than the combined object radius. This is a very stressing case due a tight turns in the relative trajectory coupled with low relative velocity. The relative velocity is below the recommended threshold for the adjoining cylinders and parallelepipeds but not for the voxels. Lack of agreement among the methods is to be expected because the slope of the cumulative probability curve is not near zero at the start of the time span. As a point of reference, the instantaneous probability at -10,800 seconds is 0.08419863. The cumulative probability (solid line in Figure A9) slope reaches zero near TCA with an instantaneous probability of 0.26952839 (dashed line). From TCA to the end of the time span the instantaneous probability slowly decreases to zero with no change in cumulative probability. This result is best understood by examining the probability density space. At TCA the combined object contains enough volume in the space to produce an instantaneous probability of 0.26952839 but nearly all that volume was already included in the cumulative calculations. As time progresses the combined object volume that was in a region of greater probability density is slowly replaced by volume of far less density, thus causing a decrease in instantaneous probability with insignificant contributions to the cumulative probability. This demonstrates that zero change in cumulative probability does not necessarily imply zero instantaneous probability.

Method	Conj Prob	diff wrt MC_e8	Other Data	Values
Monte Carlo (10e6)	0.356134000	-2.46%	Chernoff trials (1% error, 95% confidence)	1.35E+05
Monte Carlo (10e8)	0.365116060	0.00%	Dagum trials (1% error, 95% confidence)	1.80E+05
Voxels (n=50)	0.353811828	-3.10%	Combined Object Radius (m)	6
Adjoining Cylinders (n=50)	0.876788347	140.14%	Fractional Probability Threshold	0.01
Parallelepipeds (n=50)	0.397275153	8.81%	MC_e8 Fractional Probability	0.205255
Linear (Alfano n=50)	0.290078457	-20.55%		
Linear (Patera n=50)	0.290174621	-20.53%	Final Time From TCA (seconds +/-)	10800
Max Instantaneous (n=50)	0.281127866	-23.00%	Final Sigma Limit	3000
Voxels (n=100)	0.366169395	0.29%	Maximum Time Step (seconds)	5
Adjoining Cylinders (n=100)	0.876663914	140.11%	Incremental Sigma Limit	1
Parallelepipeds (n=100)	0.397222796	8.79%	Incremental angle limit (degrees)	1
Linear (Alfano n=100)	0.290146291	-20.53%		
Linear (Patera n=100)	0.290174266	-20.53%	Relative Velocity at TCA (m/s)†	0.00207874
Max Instantaneous (n=100)	0.281165135	-22.99%	Minimum Velocity needed (m/s)	0.00897895
			† motion below threshold	

Table A9: Case 9 Parameters and Results

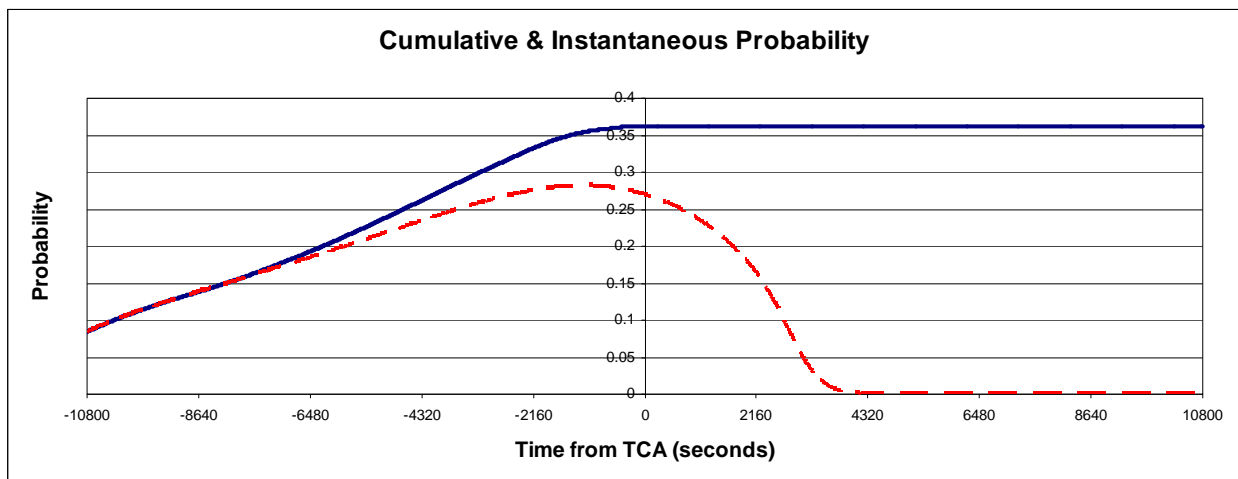


Figure A9: Case 9 Cumulative & Instantaneous Probability over Time

Case 9 A1E epoch

Primary Object ECI position (m)

-4725169.6371192000 20291999.9763030000 40356009.6612130000

Primary Object ECI velocity (m/s)

-1463.1550774022 -263.5036314079 -575.66666535477

Primary Object ECI covariance (meters & seconds)

0.0821148385670780000000 0.0075845773766415000000 0.00000000000000000000 0.00000000000000000000 0.00000000000000000000 0.00000000000000000000
0.0075845773766415000000 0.0413659274483660000000 0.00000000000000000000 0.00000000000000000000 0.00000000000000000000 0.00000000000000000000
0.0165697461308440000000 0.0029840912589638000000 0.00000000000000000000 0.00000000000000000000 0.00000000000000000000 0.00000000000000000000
0.0000000000000000000000 0.0000000000000000000000 0.0000000100000000000000 0.00000000000000000000 0.00000000000000000000 0.00000000000000000000
0.0000000000000000000000 0.0000000000000000000000 0.0000000000000000000000 0.00000001000000000000 0.00000000000000000000 0.00000000000000000000
0.0000000000000000000000 0.0000000000000000000000 0.0000000000000000000000 0.0000000000000000000000 0.0000000000000000000000 0.0000000100000000000000

Secondary Object ECI position (m)

-4725254.7737360000 20291985.4668770000 40355977.8091500000

Secondary Object ECI velocity (m/s)

-1463.1551649091 -263.5083860081 -575.6761496915

Secondary Object ECI covariance (meters & seconds)

0.0821146166791890000000 0.0075846738163084000000 0.00000000000000000000 0.00000000000000000000 0.00000000000000000000 0.00000000000000000000
0.0075846738163084000000 0.0413659693815570000000 0.00000000000000000000 0.00000000000000000000 0.00000000000000000000 0.00000000000000000000
0.0165699311713910000000 0.0029841782498233000000 0.00000000000000000000 0.00000000000000000000 0.00000000000000000000 0.00000000000000000000
0.0000000000000000000000 0.0000000000000000000000 0.0000000100000000000000 0.00000000000000000000 0.00000000000000000000 0.00000000000000000000
0.0000000000000000000000 0.0000000000000000000000 0.0000000000000000000000 0.0000000100000000000000 0.00000000000000000000 0.00000000000000000000
0.0000000000000000000000 0.0000000000000000000000 0.0000000000000000000000 0.0000000000000000000000 0.0000000000000000000000 0.0000000100000000000000

Case 9 At Time of Closest Approach (TCA, 172800 seconds after epoch)

Primary Object ECI position (m)

-5532700.6575059000 20132673.9581200000 40010548.5462730000

Primary Object ECI velocity (m/s)

-1450.9451284357 -311.6085722286 -671.3019125023

Primary Object ECI covariance (meters & seconds)

67.01362037698400000000 14.57209643865650000000 31.36298517884300000000 -0.0018373240924696000000 0.0039149399993455200000 0.0077543657627383000000
 14.57209643865650000000 3.2132921306927000000000 6.8233552264667000000000 -0.000398992190369618000000 0.0008577566771417200000 0.0016882826408446000000
 31.36298517884300000000 6.8233552264667000000000 14.7288034818100000000000 -0.0008589027630529800000 0.0018343498030328000000 0.0036389040914032000000
 -0.0018373240924696000000 -0.000398992190369618000000 -0.0008589027630529800000 0.0000000526258693147010 -0.0000001090190755636400 -0.0000002162290914182100
 0.0039149399993455200000 0.0008577566771417200000 0.0018343498030328000000 -0.0000001090190755636400 0.0000002388079993195900 0.0000004531837818429000
 0.0077543657627383000000 0.0016882826408446000000 0.0036389040914032000000 -0.0000002162290914182100 0.0000004531837818429000 0.00000009075145285822400

Secondary Object ECI position (m)

-5532694.0174556000 20132676.5073780000 40010553.8620160000

Secondary Object ECI velocity (m/s)

-1450.9465079251 -311.6078572248 -671.3005315149

Secondary Object ECI covariance (meters & seconds)

67.01428575546400000000 14.57219082072400000000 31.3631961759280000000000 -0.0018373334329171000000 0.0039149699432129000000 0.0077544252668539000000
 14.57219082072400000000 3.2133009783397000000000 6.8233774594117000000000 -0.0003989224476199200000 0.0008577596097162600000 0.0016882897157403000000
 31.3631961759280000000000 6.8233774594117000000000 14.7288543283720000000000 -0.0008589041342433800000 0.0018343579101633000000 0.0036389196118305000000
 -0.0018373334329171000000 -0.0003989224476199200000 -0.0008589041342433800000 0.0000000526259182176670 -0.0000001090193861732100 -0.0000002162297100466700
 0.0039149699432129000000 0.0008577596097162600000 0.0018343579101633000000 -0.0000001090193861732100 0.0000002388092081231000 0.0000004531861789940300
 0.0077544252668539000000 0.0016882897157403000000 0.0036389196118305000000 -0.0000002162297100466700 0.0000004531861789940300 0.00000009075192968880500

Case 10

This case involves nonlinear relative motion for two satellites in highly-eccentric orbits (HEO) and is identical to the previous case, but with a longer time span. Because of the increased time span, the slope at both ends of Cumulative Probability Chart is zero. Although the zero-slope requirement is necessary for comparison, it is not sufficient for the adjoining cylinders and parallelepipeds methods because the relative velocity is below their recommended threshold. The gaps and overlaps in the probability space are significant enough to skew the results of the adjoining cylinders method by 140%, leading to a greatly inflated cumulative probability. The parallelepiped method experiences smaller gaps and overlaps resulting in about 10% inflation. The voxel method is best able to model the collision tube and produces results that are within 1% of the Monte Carlo results. Over 192,000 Monte Carlo runs are needed for the results to be considered statistically significant. Based on the Fractional Probability Threshold of 0.01 the relative velocity at TCA is about four times less than what would be needed to drive the difference between linear and nonlinear results below 1%.

Method	Conj Prob	diff wrt MC_e8	Other Data	Values
Monte Carlo (10e6)	0.366415000	0.95%	Chernoff trials (1% error, 95% confidence)	1.46E+05
Monte Carlo (10e8)	0.362952470	0.00%	Dagum trials (1% error, 95% confidence)	1.92E+05
Voxels (n=50)	0.353811828	-2.52%	Combined Object Radius (m)	6
Adjoining Cylinders (n=50)	0.876787282	141.57%	Fractional Probability Threshold	0.01
Parallelepipeds (n=50)	0.402542132	10.91%	MC_e8 Fractional Probability	0.200517
Linear (Alfano n=50)	0.290078457	-20.08%		
Linear (Patera n=50)	0.290174621	-20.05%	Final Time From TCA (seconds +/-)	21600
Max Instantaneous (n=50)	0.281127866	-22.54%	Final Sigma Limit	3000
Voxels (n=100)	0.366169395	0.89%	Maximum Time Step (seconds)	5
Adjoining Cylinders (n=100)	0.876663914	141.54%	Incremental Sigma Limit	1
Parallelepipeds (n=100)	0.402447674	10.88%	Incremental angle limit (degrees)	1
Linear (Alfano n=100)	0.290146291	-20.06%		
Linear (Patera n=100)	0.290174266	-20.05%	Relative Velocity at TCA (m/s)†	0.00207874
Max Instantaneous (n=100)	0.281165135	-22.53%	Minimum Velocity needed (m/s)	0.00897895
			† motion below threshold	

Table A10: Case 10 Parameters and Results

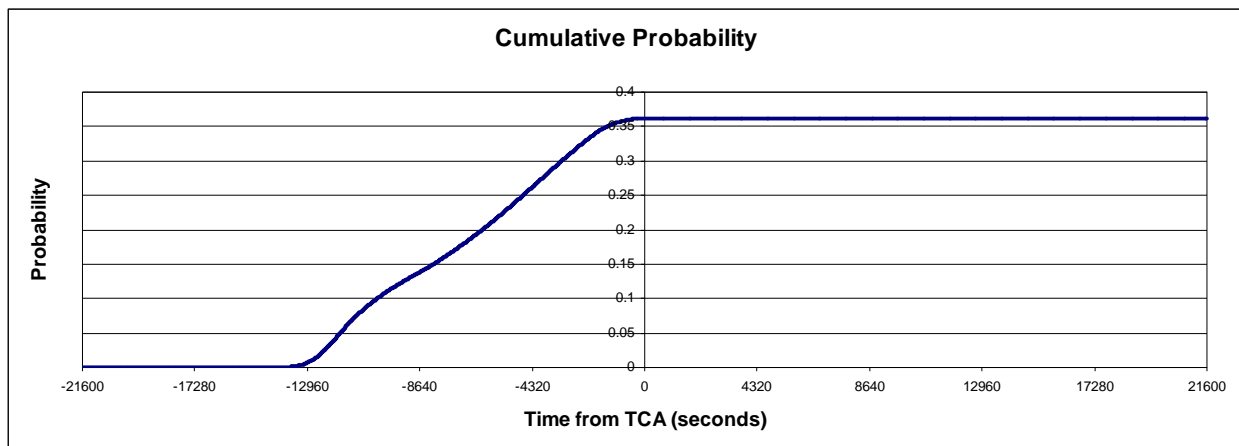


Figure A10: Case 10 Cumulative Probability over Time

Case 11

This case examines a Low-Earth Orbit (LEO) leader-follower formation where both satellites fly the same orbital path and are separated only by mean anomaly. The mean miss distance is greater than the combined object radius. Because two-body motion is modeled, the formation does not drift and there is no definitive Time of Closest Approach; TCA was arbitrarily set to one day after epoch. Although there is no relative motion in Cartesian space there is motion in the probability density space. The cumulative probability grows with time because the covariance grows; this causes the combined object to occupy different volume over time in the probability density space. The zero-slope requirement and minimum relative velocity requirement are both violated, as is the maximum instantaneous probability test. Although results for all methods are shown, none are valid for comparison. The relative motion is not sufficient for the adjoining cylinders or parallelepipeds to adequately represent the path through the probability density space; this leads to near-zero cumulative probability which is obviously below the maximum instantaneous probability. Approximately 32 million Monte Carlo runs are needed for the results to be considered statistically significant.

Method	Conj Prob	diff wrt MC_e8	Other Data	Values
Monte Carlo (10e6)	0.003400000	2.15%	Chernoff trials (1% error, 95% confidence)	1.69E+09
Monte Carlo (10e8)	0.003328530	0.00%	Dagum trials (1% error, 95% confidence)	3.20E+07
Voxels (n=50)	0.004015296	20.63%	Combined Object Radius (m)	4
Adjoining Cylinders (n=50) *	0.000000000	-100.00%	Fractional Probability Threshold	0.01
Parallelepipeds (n=50)*	0.000000000	-100.00%	MC_e8 Fractional Probability	0.197233
Linear (Alfano n=50)	0.002671975	-19.73%		
Linear (Patera n=50)	0.002672034	-19.72%	Final Time From TCA (seconds +/-)	1420
Max Instantaneous (n=50)	0.001922810	-42.23%	Final Sigma Limit	3000
Voxels (n=100)	0.003847279	15.58%	Maximum Time Step (seconds)	3
Adjoining Cylinders (n=100) *	0.000000070	-100.00%	Incremental Sigma Limit	1
Parallelepipeds (n=100)*	0.000154609	-95.36%	Incremental angle limit (degrees)	1
Linear (Alfano n=100)	0.002672026	-19.72%		
Linear (Patera n=100)	0.002672034	-19.72%	Relative Velocity at TCA (m/s)†	0
Max Instantaneous (n=100)	0.001921132	-42.28%	Minimum Velocity needed (m/s)	0.298244307
* Prob < max instantaneous value			† motion below threshold	

Table A11: Case 11 Parameters and Results

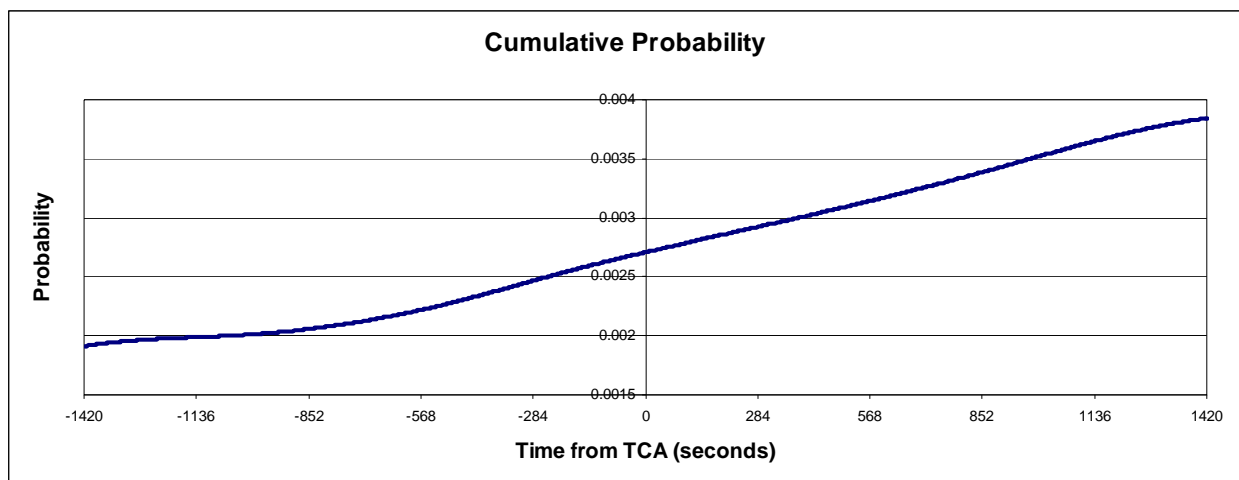


Figure A11: Case 11 Cumulative Probability over Time

Case 11 At Epoch

Primary Object ECI position (m)

6878137.0000000000 0.0000000000 0.0000000000

Primary Object ECI velocity (m/s)

0.0000000000 7612.6081732239 0.0000000000

Primary Object ECI covariance (meters & seconds)

8.5782747009869000000000 -1.3895230358788000000000 0.000000000000000000 0.000000000000000000 0.000000000000000000 0.000000000000000000
-1.3895230358788000000000 4.4217252990131000000000 0.000000000000000000 0.000000000000000000 0.000000000000000000 0.000000000000000000
0.00000000000000000000 0.00000000000000000000 4.00000000000000000000 0.000000000000000000 0.000000000000000000 0.000000000000000000
0.00000000000000000000 0.00000000000000000000 0.00000000000000000000 0.00000000000000000000 0.00000000000000000000 0.00000000000000000000
0.00000000000000000000 0.00000000000000000000 0.00000000000000000000 0.00000000000000000000 0.00000000000000000000 0.00000000000000000000
0.00000000000000000000 0.00000000000000000000 0.00000000000000000000 0.00000000000000000000 0.00000000000000000000 0.00000000000000000000

Secondary Object ECI position (m)

6878136.9995787200 76.1260818016 0.0000000000

Secondary Object ECI velocity (m/s)

-0.0842550872 7612.6081727576 0.0000000000

Secondary Object ECI covariance (meters & seconds)

8.5783054584819000000000 -1.3894770315641000000000 0.000000000000000000 0.000000000000000000 0.000000000000000000 0.000000000000000000
-1.3894770315641000000000 4.4216945415181000000000 0.000000000000000000 0.000000000000000000 0.000000000000000000 0.000000000000000000
0.00000000000000000000 0.00000000000000000000 4.00000000000000000000 0.000000000000000000 0.000000000000000000 0.000000000000000000
0.00000000000000000000 0.00000000000000000000 0.00000000000000000000 0.00000000000000000000 0.00000000000000000000 0.00000000000000000000
0.00000000000000000000 0.00000000000000000000 0.00000000000000000000 0.00000000000000000000 0.00000000000000000000 0.00000000000000000000
0.00000000000000000000 0.00000000000000000000 0.00000000000000000000 0.00000000000000000000 0.00000000000000000000 0.00000000000000000000

Case 11 At Time of Closest Approach (TCA, 86400 seconds after epoch)

Primary Object ECI position (m)	6751109.2628038000	0.0000000000	0.0000000000
Primary Object ECI velocity (m/s)	1456.2899595947	0.0000000000	0.0000000000
Primary Object ECI covariance (meters & seconds)			
	-127037.1359461200000000000000	147.096621172270000000000000	745.6801208292000000000000
	24000.0660379010000000000000	-27.780462817330000000000000	-140.8515533447200000000000
	0.000000000000000000000000	0.154247082144250000000000	0.0000000000000000000000
	-27.7804628173300000000000	0.0321769828000410000000	0.1630904203779000000000
	-140.8515533447200000000000	0.1630904203779000000000	0.8267627710686600000000
	0.000000000000000000000000	-0.0008295720219212700000	0.0000000000000000000000
Secondary Object ECI position (m)	6751123.8252900000	0.0000000000	0.0000000000
Secondary Object ECI velocity (m/s)	1456.2072604687	0.0000000000	0.0000000000
Secondary Object ECI covariance (meters & seconds)			
	-127029.9578757500000000000000	147.0886755420300000000000	745.6833077024700000000000
	23997.2540652870000000000000	-27.7772759424490000000000	-140.8436077145000000000000
	0.000000000000000000000000	0.1542470821440900000000	0.0000000000000000000000
	-27.7772759424490000000000	0.0321733727817160000000	0.1630816259934200000000
	-140.8436077145000000000000	0.1630816259934200000000	0.8267663810852000000000
	0.000000000000000000000000	-0.0008295720219208300000	0.0000000000000000000000

Case 12

This case examines two satellites co-located in identical Low-Earth Orbits (LEO). There is no drift between them and there is no definitive Time of Closest Approach; TCA was arbitrarily set to one day after epoch. There is no relative motion in Cartesian space and no motion of the combined object center in the probability density space. The cumulative probability grows with time because the covariance changes; this causes the combined object to occupy different volume over time in the probability density space. As with the leader-follower formation test case, the zero-slope requirement and minimum relative velocity requirement are both violated. There is no relative motion in the probability density space so the adjoining cylinders and parallelepipeds have no length and produce zero cumulative probability thereby failing the maximum instantaneous probability test. Although results for all methods are shown, none are valid for comparison. Approximately 42 million Monte Carlo runs are needed for the results to be considered statistically significant.

Method	Conj Prob	diff wrt MC_e8	Other Data	Values
Monte Carlo (10e6)	0.002550000	-0.23%	Chernoff trials (1% error, 95% confidence)	2.84E+09
Monte Carlo (10e8)	0.002555950	0.00%	Dagum trials (1% error, 95% confidence)	4.15E+07
Voxels (n=50)	0.003656683	43.07%	Combined Object Radius (m)	4
Adjoining Cylinders (n=50) *	0.000000000	-100.00%	Fractional Probability Threshold	0.01
Parallelepipeds (n=50)*	0.000000000	-100.00%	MC_e8 Fractional Probability	0.249795
Linear (Alfano n=50)	0.001917488	-24.98%		
Linear (Patera n=50)	0.001917487	-24.98%	Final Time From TCA (seconds +/-)	1420
Max Instantaneous (n=50)	0.001934168	-24.33%	Final Sigma Limit	3000
Voxels (n=100)	0.003079178	20.47%	Maximum Time Step (seconds)	3
Adjoining Cylinders (n=100) *	0.000000000	-100.00%	Incremental Sigma Limit	1
Parallelepipeds (n=100)*	0.000000000	-100.00%	Incremental angle limit (degrees)	1
Linear (Alfano n=100)	0.001917487	-24.98%		
Linear (Patera n=100)	0.001917487	-24.98%	Relative Velocity at TCA (m/s)†	0
Max Instantaneous (n=100)	0.001932488	-24.39%	Minimum Velocity needed (m/s)	0.087688497
* Prob < max instantaneous value			† motion below threshold	

Table A12: Case 12 Parameters and Results

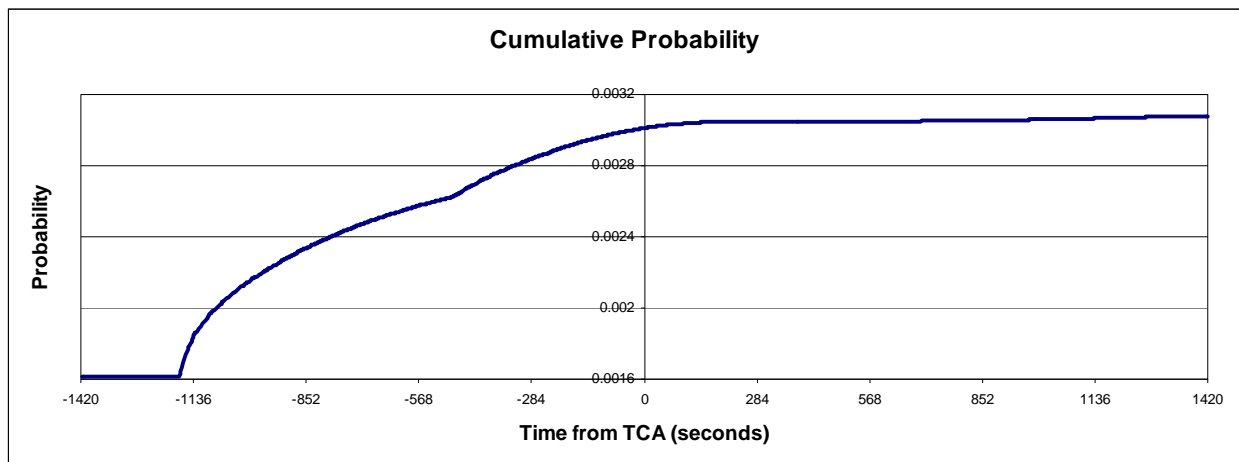


Figure A12: Case 12 Cumulative Probability over Time

Case 12 At Epoch

Primary Object ECI position (m)

6878137.0000000000 0.0000000000 0.0000000000

Primary Object ECI velocity (m/s)

0.0000000000 7612.6081732239 0.0000000000

Primary Object ECI covariance (meters & seconds)

8.5782747009869000000000 -1.3895230358788000000000 0.0000000000000000000000 0.0000000000000000000000 0.0000000000000000000000 0.0000000000000000000000
-1.3895230358788000000000 4.421725299013100000000000 0.0000000000000000000000 0.0000000000000000000000 0.0000000000000000000000 0.0000000000000000000000
0.0000000000000000000000 0.0000000000000000000000 0.0000000000000000000000 0.0000000000000000000000 0.0000000000000000000000 0.0000000000000000000000
0.0000000000000000000000 0.0000000000000000000000 0.0000000000000000000000 0.0000000000000000000000 0.0000000000000000000000 0.0000000000000000000000
0.0000000000000000000000 0.0000000000000000000000 0.0000000000000000000000 0.0000000000000000000000 0.0000000000000000000000 0.0000000000000000000000
0.0000000000000000000000 0.0000000000000000000000 0.0000000000000000000000 0.0000000000000000000000 0.0000000000000000000000 0.0000000000000000000000

Secondary Object ECI position (m)

6878137.0000000000 0.0000000000 0.0000000000

Secondary Object ECI velocity (m/s)

0.0000000000 7612.6081732239 0.0000000000

Secondary Object ECI covariance (meters & seconds)

8.5782747009869000000000 -1.3895230358788000000000 0.0000000000000000000000 0.0000000000000000000000 0.0000000000000000000000 0.0000000000000000000000
-1.3895230358788000000000 4.421725299013100000000000 0.0000000000000000000000 0.0000000000000000000000 0.0000000000000000000000 0.0000000000000000000000
0.0000000000000000000000 0.0000000000000000000000 0.0000000000000000000000 0.0000000000000000000000 0.0000000000000000000000 0.0000000000000000000000
0.0000000000000000000000 0.0000000000000000000000 0.0000000000000000000000 0.0000000000000000000000 0.0000000000000000000000 0.0000000000000000000000
0.0000000000000000000000 0.0000000000000000000000 0.0000000000000000000000 0.0000000000000000000000 0.0000000000000000000000 0.0000000000000000000000
0.0000000000000000000000 0.0000000000000000000000 0.0000000000000000000000 0.0000000000000000000000 0.0000000000000000000000 0.0000000000000000000000

